

## 9. VALLEY CALCULATIONS USING EXTRAORDINARY RAY DATA

### 9.1 Introduction

Cusp type discontinuities on an ionogram are normally caused by a peak or local maximum in the electron-density profile. Reflections are not obtained from the region of decreased density above a peak, so that there is an unobserved region (called a valley) between observed ionospheric layers. The width of the valley is the height range over which the plasma frequency is less than the value at the underlying peak. The valley depth gives a measure of the amount by which the plasma frequency in the valley is less than the peak value. For accurate calculations of the real heights at higher frequencies we need to know the width and depth of the valley, and (when the valley depth is not small) the approximate shape of the profile in the valley region. There is no analytic procedure which can obtain this information from a single  $h'(f)$  trace. When only ordinary ray data are available we must therefore use some model for the valley region, as discussed in Section 7.

When both ordinary and extraordinary ray data are available at frequencies slightly above the critical frequency of the lower layer, some information about the valley can be obtained from an ionogram. In theory, and neglecting the variation of gyrofrequency with height, corresponding sections of the two traces (i.e. sections corresponding to the same range of plasma frequencies at reflection) can be used to determine exactly the effect of the valley. Such an exact solution would give the true heights for the upper layer, and all moments of the ionisation in the valley. In practice, however, only one or two valley parameters can be determined. This is similar to the problem in defining the underlying ionisation at the start of an analysis, as discussed in Section 8.1. Additional problems appear at dip angles near  $30^\circ$ , where only a single parameter can be determined, and at dip angles near  $35^\circ$  where practical X-ray calculations become almost impossible (Appendix B.2).

With the accuracy of current ionosondes only one parameter can normally be determined (Lobb and Titheridge, 1977a). Attempts to determine additional parameters do not yield any increase in accuracy and have two undesirable consequences.

- (1) Using a given amount of data, additional valley information is obtained basically by placing additional constraints on the observed part of the profile. This generally gives a less satisfactory solution, with an unphysical valley distribution and (if the total number of parameters being determined is held constant) an increase in the RMS error with which the virtual heights are fitted.
- (2) Too much flexibility in the unobserved (and therefore ill-defined) valley region leads to less stability in the solution. Small changes in any of the data points, changes in the number of data points used in the valley solution, or changes in the total number of parameters determined, can then cause large variations in the calculated real heights in the observed region.

Both effects have been demonstrated in Section 8 when considering the starting problem; use of the two-parameter slab start in place of the more flexible polynomial start gives an improvement in the accuracy with which the virtual heights are fitted, and halves the variation in the calculated heights between different modes of analysis. In valley calculations using practical ionograms, different assumptions about the valley shape give calculated widths varying by about 15% (Titheridge, 1959b and later calculations). Errors in the calculated F-region heights are a similar percentage of the uncorrected error. Thus only a one-parameter valley calculation is normally feasible, and this reduces the errors in calculated F-layer heights by a factor of about 5. For most work, optimum accuracy and reliability are achieved by the use of a fixed but reasonably sophisticated model for the valley shape.

The parameter of most importance in valley calculations is the width of the valley. This should therefore be the single parameter which is determined. For optimum results the valley model should define reasonable values for other parameters which affect the overall group retardation; these are the curvature above the peak of the lower layer, the mean electron density in the valley, and the electron density gradient at the upper edge of the valley. The profile obtained will then be physically reasonable in all important aspects. The one-parameter analysis selects one of a single family of valleys, of similar shape but differing in width. This family is based on the "Standard Valley" used in ordinary-ray analysis and described in Section 7.2. A wide range of different forms for the valley region can be obtained, if required for particular studies, by suitable choice of the input parameter VALLEY as described in Section 10.2.

Calculations using a single polynomial representation for the upper part of the valley and the lower part of the F layer give more variable results, because of the greater variability which is possible in the unobserved valley region. The same problem arises if the valley region is represented by a number of parabolic sections of arbitrary gradient and curvature (as in Howe and McKinnis, 1967);

this gives physically impossible valley distributions in most cases, with unacceptable errors in the calculated real heights at higher frequencies. At the other extreme use of a simple triangular valley (as in the simplified program SPOLAN) is found to give good results under most conditions but, since it does not provide a realistic amount of group retardation, is less accurate if virtual-height data are used at frequencies within about 0.05 MHz of the critical frequency of the lower layer.

## 9.2 The Normal Analysis - Calculation of Valley Width.

The model adopted for the valley shape is shown in Fig. 17. For a given valley depth the real-height profile in the valley region is defined by three sections:

- (i) A parabolic section extending from the peak of the lower layer to the depth VDEPTH. This section has a scale height 40% greater than that calculated from the virtual-height data for the lower layer. The parabolic section covers a height interval PARHT which depends only on VDEPTH and the scale height (as described in Section 7.2).
- (ii) A slab of ionisation with a constant plasma frequency FC-VDEPTH extending over a height range  $0.6q(JM)$ , where  $q(JM) = VWIDTH - PARHT$ .
- (iii) A section in which the electron density increases linearly with height (and FN increases from FC-VDEPTH to FC) in a distance  $0.4q(JM)$ .

For an E layer with HMAX = 120 km, the standard valley used in the absence of X-ray data has an overall width of 20 km and a depth of 0.08 MHz. This is described in Section 7, and shown by the thick line in Fig. 17. For wider valleys the depth is increased to maintain a reasonable shape for the valley region. At small values of VWIDTH the depth is varied as  $(VWIDTH)^2$ , while for larger widths the depth becomes proportional to width (as described in Section 7.2). This gives acceptable values for both the mean depth and the gradient  $dFN/dh$  at the top of the valley, and provides a single family of standard valleys as shown in Fig. 17.

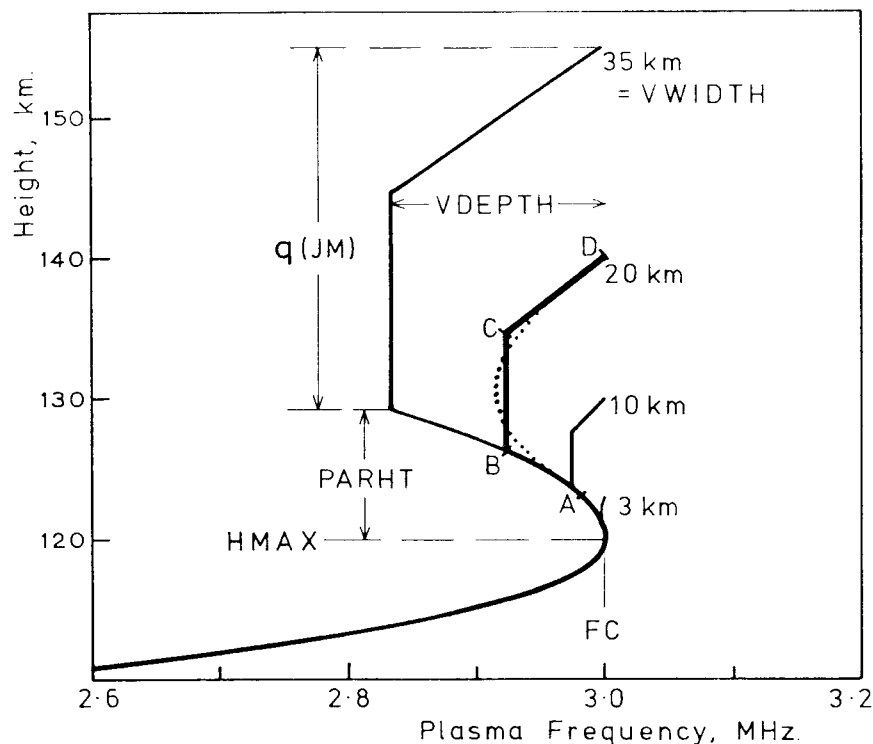


**Figure 17.** The shape of the standard valley, for different values of the single parameter VWIDTH. The dotted line shows a possible form for the true variation of plasma frequency with height in an E-F valley; this will give (very closely) the same virtual heights as the solid line model. A to D show the four points which are added to the calculated real height data, to define the valley region.

The models in Fig. 17 are a reasonable match to the valleys obtained by superposing two Chapman layers, and give similar gradients at the top of the valley. The valley depths are slightly less than those obtained with superposed Chapman layers; however the Chapman models allow for only two distinct production mechanisms with no other ionisation sources acting between the layers. Back-scatter measurements suggest that the valley profile is rarely a simple curve with a single minimum, and may generally be closer to the flat-bottomed shape given by the continuous lines in Fig. 17.

A least-squares calculation of valley width is possible only if the valley depth VDEPTH is first specified. An iterative procedure is therefore required, to maintain the fixed relation between valley depth and valley width. Calculations start by assuming VWIDTH = HMAX/2-40 km, where HMAX is the height of the underlying peak (as in Section 7.2). The corresponding depth is obtained from

$$VDEPTH = 0.008 VWIDTH^2 / (20 + VWIDTH) \text{ MHz} \quad (14a)$$

followed by

$$VDEPTH = VDEPTH.FC / (VDEPTH + FC) \quad (14b)$$

to ensure that the depth remains less than the critical frequency FC of the lower layer. Polynomial coefficients can then be calculated, and a least-squares analysis used to determine the value of VWIDTH which gives the best fit to the ordinary and extraordinary ray virtual-height data. A revised estimate of the depth is then obtained from the above relations, and the analysis repeated to obtain a new value of VWIDTH. Virtual heights depend primarily on the width of the valley, so the calculated width changes by only about 10% (in a typical case) for an increase of four times in the assumed depth. Thus a third calculation, after a second adjustment of the valley depth using (14), is sufficiently accurate to be used as the final result.

At each stage of the calculation the RMS fitting error, between the given virtual-height data and the virtual heights corresponding to the calculated profile, is obtained. If in the second or third calculation this error shows a significant increase, the previous calculation is adopted as the correct answer. This check will, for instance, prevent the valley depth from being increased above 0.05 MHz when analysing data corresponding to a wide but abnormally shallow valley. A "significant" increase in the error parameter DEVN is currently defined in POLAN to be an increase of more than 10%. Smaller increases commonly result from inaccuracies in the data, and do not provide a sufficiently clear indication to justify departures from the normal valley shape.

For each assumed depth, the calculation of valley width proceeds as follows. The real-height profile for the bottom of the upper layer is defined by a polynomial which includes a constant term, giving

$$h - HA = \sum_{j=1}^{NT} q(j) \cdot (FN-FA)^j + q(JM) \quad \text{where} \quad JM = NT+1.$$

The origin for this polynomial is at FA = FC and HA = HMAX+PARHT. The virtual-height equations of Section 4.2 then become

$$h''(k+i) - HA = \sum_{j=1}^{JM} q(j) \cdot B(i,j)$$

where B(i,JM) gives the delay for a valley section (B to D in Fig. 17) of unit thickness. The least-squares solution of these equations, which include both ordinary and extraordinary ray frequencies, gives (i) the normal parameters q(1) to q(NT), which define the polynomial section at FN > FC, and (ii) the value of q(JM) which raises the starting height of the polynomial.

Results obtained depend sensitively on the value of the gyrofrequency FB used in the calculation, since this affects not only the values of  $\mu'$  but also the plasma densities at which the extraordinary rays are reflected. For calculating the delay in the valley region, the gyrofrequency at the height HMAX is used. If NX is the number of X-ray virtual heights employed in the analysis, the gyrofrequency used when integrating  $\mu'$  over the upper polynomial section corresponds to the height of reflection of the ray number 1 + NX/3. This height FHHT is the height of reflection of the first X-ray if NX = 1 or 2, the second X-ray for NX = 3, 4 or 5, and so on. The correct value of FHHT is not known at the start, so calculation of the coefficients B(i,j), the parameters qj and the height of reflection FHHT is iterated until FHHT changes by less than 2 km. (The maximum allowed change is set by the parameter HXERR in a DATA statement in the subroutine STAVAL.)

### 9.3 Calculation of Valley Width and Depth

With accurate virtual-height data and a reasonable model for the shape of the valley region, it is sometimes possible to obtain more accurate results by determining two parameters for the valley region. In all numerical tests using exact model ionograms, a two-parameter analysis as described below is feasible and yields results of good accuracy. If typical experimental errors are introduced, however, the usefulness of a two-parameter analysis becomes doubtful. This problem has been discussed elsewhere (Lobb and Titheridge, 1977a) where it is shown, for example, that an error of 1% in the estimated value of the critical frequency of the lower layer makes determination of a second valley parameter unreliable. In such cases it is better to use the one-parameter analysis, determining only the valley width and assuming some physically reasonable shape for the valley. Attempts to determine two valley parameters from inexact data generally gives less accurate results, for both the valley region and the height of the upper layer, than use of a single-parameter analysis. This confirms the general philosophy of Section 8.1, adopted in POLAN, that the number of parameters used to represent the unobserved regions of the ionosphere should be kept to a minimum.

The least-squares valley calculation used in POLAN provides directly the RMS error  $DEVN$  between the given virtual-height data and the virtual heights corresponding to the calculated profile. In most practical work the one-parameter valley calculation of Section 9.2 yields values of  $DEVN$  which are less than the experimental error in the virtual heights. The resulting profile then fits the observations to within experimental error and no further information can be obtained. In some cases, however, using carefully selected ionograms and careful scaling, the values of  $DEVN$  may be greater than the expected experimental error. This suggests that the actual valley shape departs significantly from the one-parameter model. Increased accuracy in the calculated real heights, and additional information about the valley, may then be obtainable. For this purpose an iteration with different valley depths can be used to minimize  $DEVN$  and obtain a second valley parameter. The procedure described below appears to be about optimum for obtaining two independent parameters, since the valley model incorporates no unnecessary features and so maintains a physically reasonable shape at all times. It should be emphasized, however, that this analysis is recommended only for specific studies of carefully selected ionograms. Routine determination of two parameters will not be possible until ionograms give a meaningful accuracy of better than about 0.05% in frequency and 0.5 km in height. A discussion of typical errors with current ionosondes is given by Koehler and McNamara (1975).

A parameter  $VALLEY$  is included in the call to the  $N(h)$  analysis subroutine POLAN. This is zero or one for a normal analysis. Other values can be used to redefine the standard valley inserted in an ordinary ray analysis (Section 7.4), and the shape of the valley used in a one-parameter valley analysis. If POLAN is called with  $VALLEY = -1.0$ , and adequate X-ray data are provided, the valley width and depth are determined independently. For each value of  $VWIDTH$  there is a family of allowed valleys, as shown in Fig. 18. Independent calculation of the two parameters  $VWIDTH$  and  $VDEPTH$  involves the following steps.

- (a) The valley depth  $VDEPTH$  is set equal to 0.1001 MHz. The real and virtual height coefficients (Section 4.2) are then calculated by the subroutine  $COEFIC$ , and the corresponding real-height coefficients obtained by the subroutine  $SOLVE$ . Keeping the same value of  $VDEPTH$  this solution is iterated (as described in Section 9.2) until the height  $FHHT$  used to define the gyrofrequency near reflection changes by less than 2 km.
- (b) The calculations in (a) are repeated using  $VDEPTH = 0.6006$  MHz. (Odd values of depth are used so that these preliminary cycles can be clearly identified within POLAN).
- (c) Results from (a) and (b) are compared, and valley depth iteration begins from whichever value of  $VDEPTH$  gave the best fit to the virtual-height data (i.e. the smallest value for the RMS fit error  $DEVN$ ). This preliminary selection of a starting point for the iteration of  $VDEPTH$  is used to avoid spurious minima in  $DEVN$ , as discussed in Section 9.4 below.
- (d) The valley depth  $VDEPTH$  is multiplied by a factor  $DVAL = 1.0 + 0.5 \cos(0.86DIP)$ . This changes the depth by a factor of 1.5 at low latitudes, dropping to 1.2 at high latitudes where the minima in  $DEVN$  are narrower. Calling of  $COEFIC$  and  $SOLVE$  then gives new values for the valley width  $VWIDTH$  and the fitting error  $DEVN$ . If  $DEVN$  is increased compared with the previous calculation then the values of  $VWIDTH$  and  $DEVN$  from steps (c) and (d) are exchanged, and  $DVAL$  is replaced by  $1/DVAL$  so that the depth will decrease on successive iterations.
- (e)  $VDEPTH$  is multiplied by  $DVAL$  and the analysis repeated to give new values of  $VWIDTH$  and of  $DEVN$ . This step is repeated until  $DEVN$  stops decreasing (or decreases by less than 3% between successive steps; possibly because of a broad, ill-defined minimum).
- (f) At this stage we use the last three values of  $VDEPTH$ , which differ by the factor  $DVAL$ , and the corresponding values of  $DEVN$ . Second difference interpolation is applied to these results to determine the exact depth for which the error would be a minimum. If  $DEVN$  had begun to increase, this minimum will be in the range of the last three values of  $VDEPTH$ . If the bracketed condition in (e)

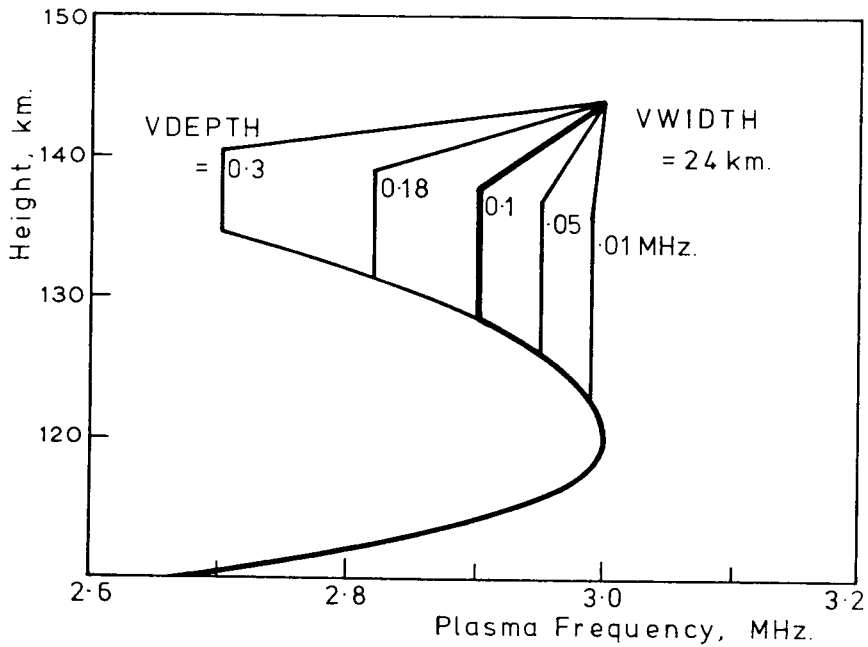


**Figure 18.** Variations in the model valley, obtained by changing the valley depth VDEPTH at a fixed value of valley width. The heavy line shows the "standard" relation between depth and width, as assumed in the one-parameter analysis of Section 9.2.

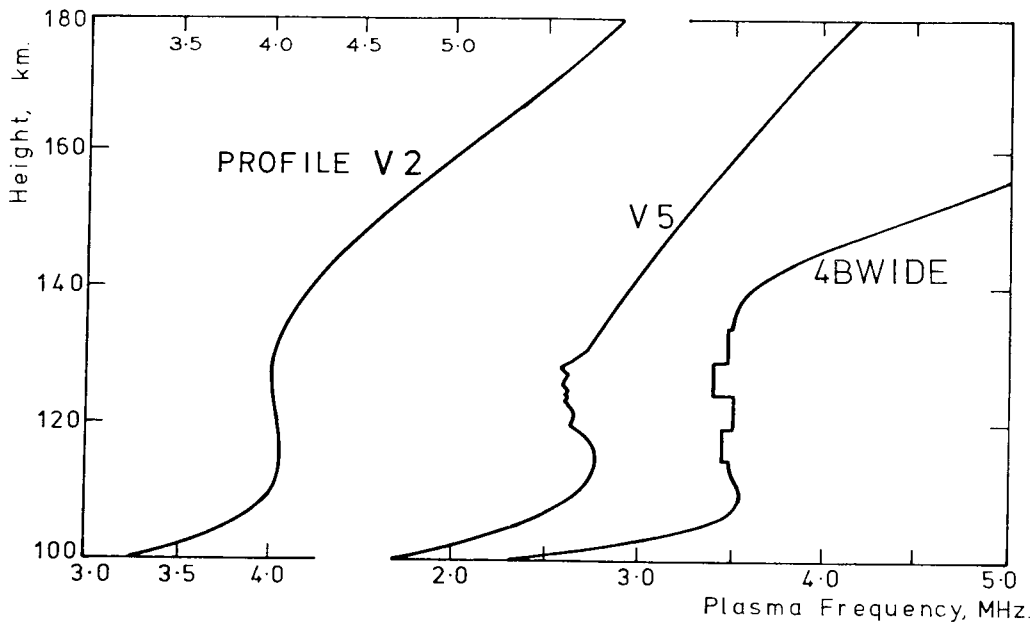


**Figure 19.** Three of the many profiles used to investigate valley calculation procedures. V2 and V5 correspond to the valley profiles 2 and 5 used in the URSI tests (and described in McNamara and Titheridge, 1977). Profile 4BWIDE originated as overlapping Chapman layers, giving a 20-km wide valley with a depth of 0.055 MHz. Four slabs of constant density were then added at the bottom of the valley; each slab covered a height range of 5 km and the plasma frequencies were 0.04, 0.08, 0.10 and 0.15 MHz less than the E-layer critical frequency ( $f_oE = 3.53$  MHz).

had been employed, however, the minimum may be outside this range; it is not allowed to extend more than an additional factor of  $DVAL \cdot 5$ . When the depth corresponding to minimum DEVN is determined, one further calculation gives the final values for the width of the valley and the RMS fitting error.

At each stage the width and depth of the valley, the value of DEVN and the number of terms and frequencies used in the analysis are listed. The total number of iterations (including the inner loop which is used at each step to reach a correct value of FHHT) is also counted and listed; if this count reaches 25 the iteration is abandoned. At the completion of the valley calculation the points A to D in Fig. 17 are added to the real-height array, followed by the real heights for the upper layer.

Checks similar to those described in Section 7.3.3 are applied to ensure that a physically reasonable result is obtained. The first check is carried out at each step, to ensure that the gradient of the polynomial section (from D in Fig. 17) is greater than 2.0 km/MHz. If a bad value occurs, the weight given to the X-ray data is reduced (by a factor of 4) and the analysis repeated. If the profile gradient is still too small the solution is modified by reducing the offset term  $q(JM)$ ; this lowers the starting point (D in Fig. 17) for the real-height polynomial. With some types of contradictory O and X data this can fail to increase the gradient at higher frequencies; the message "DATA AND GYROFREQUENCY INCOMPATIBLE AT F = xx.xx" is then printed, and no further valley iterations are attempted.

If the distance  $q(JM)$  is less than  $PARHT/2$  (Fig.17) the weight given to the X-ray data is decreased, the value of VDEPTH is halved, and a new solution is obtained. Halving of VDEPTH and recalculation of  $q(JM)$  is repeated until  $q(JM) > PARHT/2$ . This ensures a physically reasonable shape for the final valley region. The variations obtained as the depth of the valley changes, at a fixed value of valley width, are shown in Fig. 18.

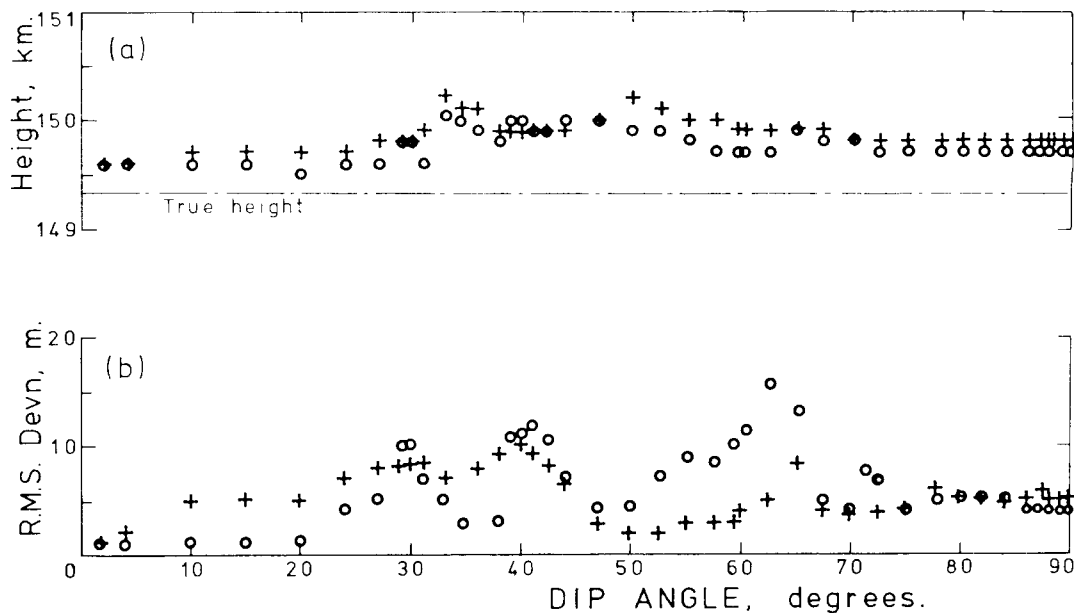
#### 9.4 Results With Test Model Ionograms

In the absence of X-ray data, POLAN inserts a defined "standard valley" between successive ionospheric layers. The size and depth of this valley depend on the height of the underlying peak, as described in Section 7.2. When X-ray data are provided (and the parameter VALLEY is zero or one) a valley is selected from the family shown in Fig. 17. Selection is done essentially by determining the width that gives the smallest RMS deviation (DEVN) between the given virtual-height data and virtual heights corresponding to the calculated profile. To calculate the width we must assume some value for the valley depth. Results are iterated, adjusting the depth to maintain the standard relation between valley depth and width, to obtain a final result of the type shown in Fig. 17.

Errors in the resulting profile, due to differences between the true and assumed shape of the valley region, can be estimated by repeating the calculations for different (fixed) values of valley depth. Calculations of this type have been carried out for a wide range of different valley profiles. Fig. 19 shows three of the profiles used, for which results are described below. Profile V2 gives a smooth analytic variation obtained with two overlapping Chapman layers. The valley region in V5 contains much irregular structure, corresponding to variations measured on one occasion by the Arecibo backscatter sounder. 4BWIDE represents a particularly difficult type of profile; the wide, shallow valley contains large, semi-random variations in density, and above the valley region the profile gradient changes rapidly.

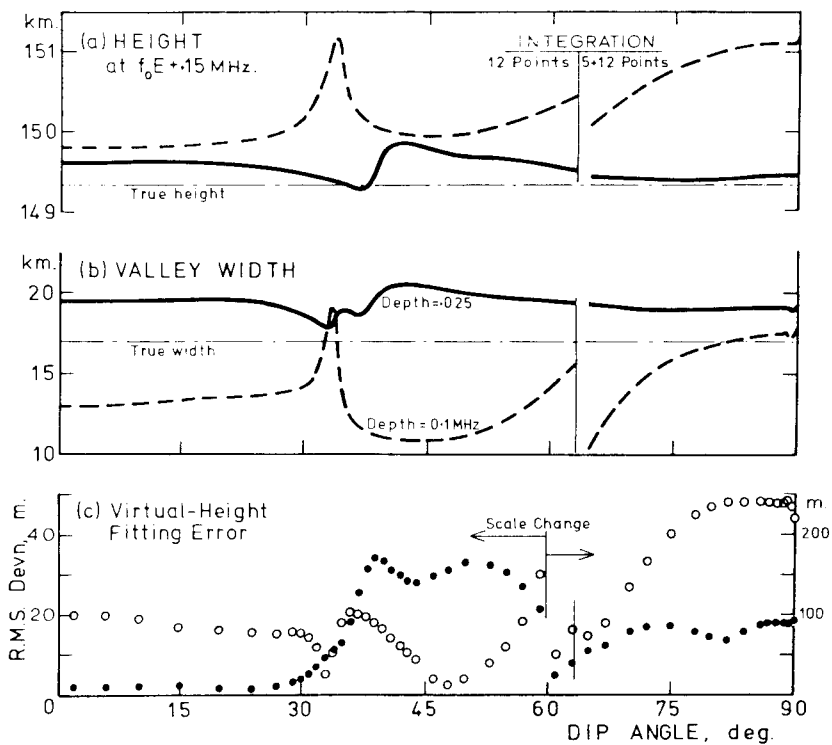
All calculations described in this section were carried out without including any of the "physical constraints" described in Section 7.3, so the results shown represent a purely mathematical solution to the valley problem. The physical constraints, normally included in the set of least-squares equations solved by POLAN, affect the results to a varying degree. With good data, and dip angles not near  $30^\circ$ , there is a sharp minimum in the variation of virtual-height fitting error with valley depth (as at dip =  $75^\circ$  in Fig. 22(a)). This gives a well-defined solution for the valley region. Inclusion of the physical constraints then increases the RMS fitting error but produces little change in the calculated profile. Where the virtual-height error varies only slowly with the assumed shape of the valley (as at dip =  $30^\circ$  in Fig. 22(a)) the data do not give a clearly-defined valley. Inclusion of the physical constraints then gives a profile which tends towards the "standard" values of depth and width, since this change produces little increase in the virtual-height fitting error.

Figure 20 summarises the results of analysing accurate virtual-height data calculated from profile V2, at 41 different dip angles. A frequency interval of 0.05 MHz was used above the critical frequency of the lower layer (at  $foE = 4.05$  MHz). The full iterative 2-parameter analysis of Section 9.3 was applied to determine valley width and depth independently, for two different modes of POLAN. Results fit the virtual-height data to within about 0.01 km (Fig. 20b) so that use of a more sophisticated valley model, corresponding to the introduction of a third valley parameter, can not be justified. The calculated real heights just above the valley are about 0.2 to 0.7 km too large (Fig.



**Figure 20.** Results from two-parameter valley calculations using accurate virtual-height data corresponding to profile V2. o and + show the results obtained using two different modes (5 and 6) in POLAN.

- (a) The calculated height above the valley, at a plasma frequency  $F_N = f_oE + 0.15$  MHz.
- (b) The accuracy with which the calculated profile fits the virtual-height data.



**Figure 21.** Analysis of the virtual-height data from profile V2, which has an effective valley depth of about 0.04 MHz. Results shown were calculated using fixed valley depths of 0.025 MHz (solid lines and dots), and 0.1 MHz (broken lines and circles). The discontinuity at 63° dip is due to the change in POLAN to a double-integration procedure at high dip angles (as discussed in Appendix B.3).

20a). This represents the achievable limit of accuracy in valley calculations. At higher frequencies the errors decrease smoothly, approximately as  $1/f^2$ , as shown in Fig. 9 of Section 7.4.

Results for a one-parameter calculation of valley width only, assuming a fixed value of valley depth, are shown in Fig. 21. Solid lines and dots are the results obtained assuming a valley depth of 0.025 MHz - about half the true value - while broken lines and circles are for an assumed valley depth of 0.1 MHz. For one-parameter calculations the results obtained from modes 5 and 6 of POLAN are very similar, and Fig. 21 gives the mean values from both modes. Calculations were repeated for 47 different dip angles, plotted individually in Fig. 21(c), to define adequately the fluctuations near dip  $34^\circ$  and at high dip angles.

The virtual-height fitting errors are considerably greater in Fig. 21(c) than in Fig. 20(b). The increase is by a factor of about 30 at high dip angles, where the RMS deviation varies rapidly with the assumed valley depth (as shown in Fig. 22 below). The mean virtual-height error in Fig. 21(c) increases by a factor of about 5 from middle to high latitudes, while the real-height error increases by a factor of about 2. At dip angles between about  $30^\circ$  and  $40^\circ$  the real-height errors tend to increase, and change rapidly with dip angle. This effect is studied in Appendix B.2. It occurs with all profiles, and prevents useful X-ray calculations being made at dip angles near  $35^\circ$ .

The calculated valley widths in Fig. 21(b) are typically 25% too small at  $VDEPTH = 0.1$  MHz, and 15% too high at  $VDEPTH = 0.025$  MHz. This gives real-height errors of about  $\pm 3$  km at the top of the valley (where the plasma frequency  $f_N$  is equal to the value  $f_oE$  in the underlying peak). The calculated gradients at this point also vary, in the opposite direction, so that the real-height error decreases rapidly just above the valley. At a plasma frequency of  $f_oE + 0.15$  MHz, near the centre of the frequency range used in the valley calculation, the mean real-height error is about +0.5 km. This error remains between 0.0 and +1.0 km at most dip angles, for any value of  $VDEPTH$  within a factor of two of the correct value.

The effects of changes in the assumed valley depth are shown in detail in Fig. 22. Virtual height data corresponding to profile V5 at dip angles of  $30^\circ$  and  $75^\circ$  (from McNamara and Titheridge, 1977) were analysed using a total of 110 different values for the valley depth  $VDEPTH$ . Each calculation corresponds to a single pass through the valley calculation in POLAN, without iteration and without the "physical constraints" normally included in the least-squares solution. Eight parameters, corresponding to the valley width  $VWIDTH$  and a 7-term polynomial for the reflecting region, are determined by a least-squares fit to the first 6 O-ray and 6 X-ray virtual heights. These heights are for plasma frequencies (at reflection) at intervals of 0.05 MHz above the critical frequency  $f_oE$  of the lower layer.

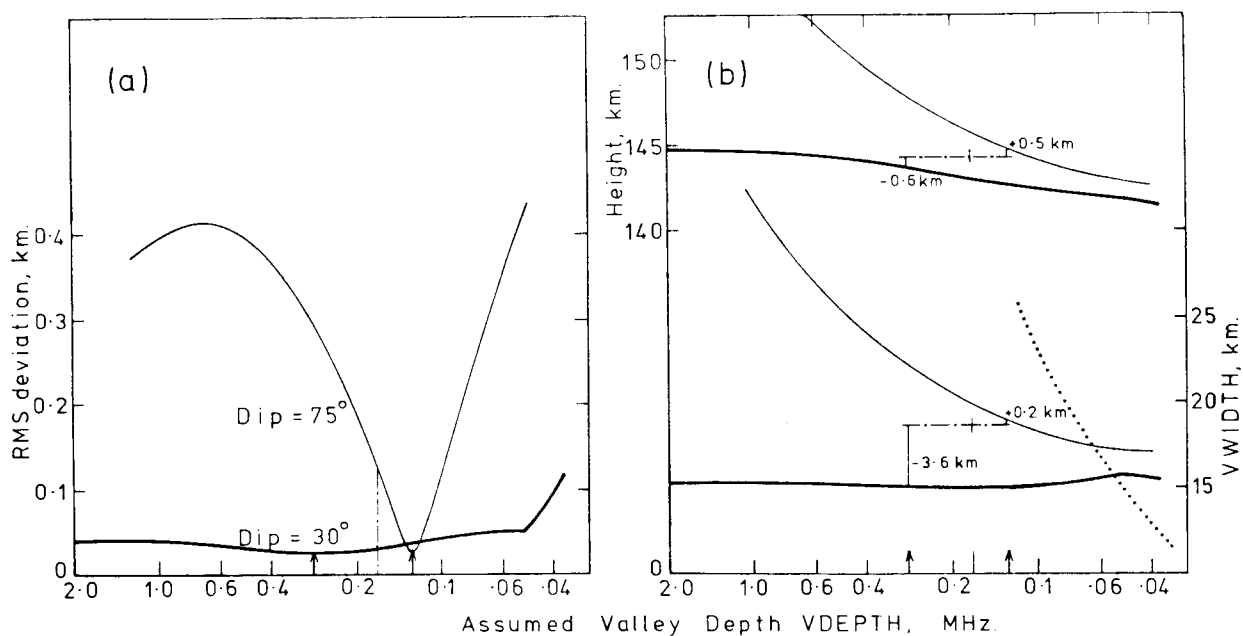


**Figure 22.** Analysis of virtual-height data corresponding to the profile V5, at two values of dip angle, using different assumed values for the valley depth. Ordinary and extraordinary ray data were used at six frequencies, corresponding to plasma frequencies at reflection from  $f_oE + 0.05$  MHz to  $f_oE + 0.3$  MHz in steps of 0.05 MHz. Chain lines show the true values of  $VDEPTH$ ,  $VWIDTH$  and real height (at  $f_oE + 0.3$  MHz). Arrows mark the values corresponding to a minimum in the RMS virtual-height fitting error.



The curves in Fig. 22(a) give the RMS deviation with which the best profile, for a given assumed valley depth, fits the 12 virtual-height data points. At dip  $75^\circ$  (fine line) there is a clearly defined minimum deviation, at a depth VDEPTH of 0.13 MHz. This is less than the approximate mean depth of 0.17 MHz for the valley in profile V5. Since, however, profile V5 differs considerably from the POLAN model, and fluctuates considerably in the valley region, this difference is not very significant. Fig 22(b) shows that the valley width corresponding to the minimum deviation is accurate to within 1%, and the calculated real height at  $foE + 0.3$  MHz is accurate to 0.5 km.

Incorrect values of VDEPTH typically give virtual-height fitting errors of about 0.3 km at a dip angle of  $75^\circ$ . The valley width and the calculated heights of the lower F layer have errors of several km. These results are representative of the many different profiles studied. The dotted curve in Fig. 22(b) shows the relation between valley depth and width assumed by the "standard valley" model used for a one-parameter analysis. The intercept between this curve and the lower continuous curves in Fig. 22(b) defines the depth which would be assumed in the one-parameter analysis. This depth is 0.065 MHz at dip  $75^\circ$ , giving errors of -1.1 km in valley width and -1.0 km in F-layer height (at  $foE+0.3$  MHz).

At dip  $30^\circ$  little information can be obtained about the valley depth. The virtual-height data can be fitted with a maximum RMS error of 0.04 km for all valley depths from 2.5 to 0.05 MHz, as shown by the heavy line in Fig. 22(a). (The increase at small depths is caused by the check in POLAN which disallows a negative value of  $dh/dFN$  above the valley). With normal data, calculated profiles fit the data to a high degree of accuracy for any reasonable valley depth. The calculated value of VWIDTH, shown by the lower solid curve in Fig. 22(b), is almost independent of the assumed depth. The real height at  $foE+0.3$  MHz (upper curve) also varies only slowly with depth; for any assumed depth between 2.5 and 0.05 MHz this error is between +0.5 and -2.5 km. The error of 0.6 km corresponding to the profile with smallest RMS deviation is approximately the same as for the  $75^\circ$  case.

These results confirm that for dip angles between about  $26^\circ$  and  $30^\circ$  the distribution of ionisation in the unseen regions cannot be found reliably, so that only a single-parameter valley calculation is justified (Appendix B and Titheridge, 1974b). The poor determination of valley shape does not, however, reduce the accuracy of calculated real heights in the observed frequency range. The results shown use data at frequency intervals  $\Delta f$  of about 0.05 MHz above  $foE$ , representing the closest scaling which is reasonable in most practical cases. Increased accuracy can be obtained, with the model data, by reducing  $\Delta f$  to 0.03 MHz; this gives real-height errors at  $foE+0.3$  MHz of less than 0.1 km for both dip angles.

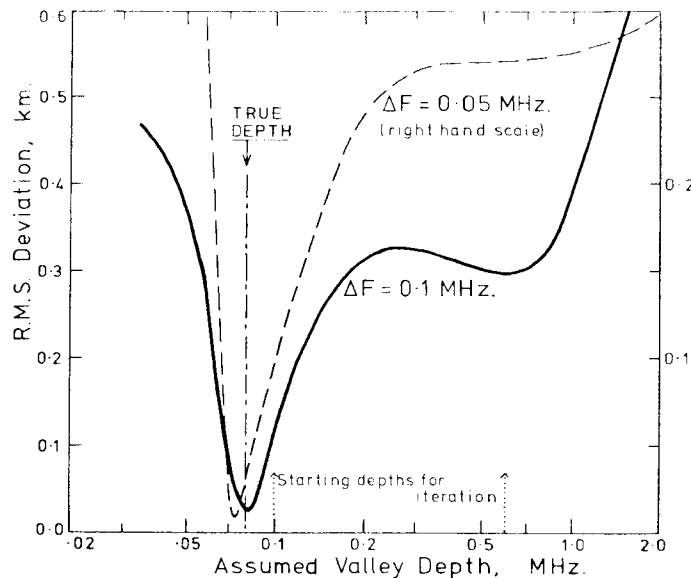


**Figure 23.** The variation of virtual-height fitting error with the assumed valley depth, for calculations at a dip angle of  $52^\circ$  and frequency intervals  $\Delta f$  of 0.1 and 0.05 MHz.

We conclude from these studies that for most work the valley region should be represented by only one parameter, to select one valley from some physically-reasonable family. Real-height errors above the valley will then be roughly 10 to 20% of the valley width. This assumes the existence of good virtual-height data, for both the ordinary and extraordinary rays, at frequencies near  $f_oE+0.1$  MHz. With excellent data, and at dip angles outside the range  $25^\circ$  to  $38^\circ$ , use of a second valley parameter (which represents basically the mean depth of the valley) can reduce real-height errors to a few percent of the valley width.

In some cases the virtual-height fitting error plotted as a function of VDEPTH does not have a single minimum. This occurs most often at medium to high dip angles, and with wide, shallow valleys. Results for profile 4BWIDE analysed at dip  $52^\circ$  are shown in Fig. 23. Calculations used 6 virtual heights, for each component, at frequency intervals  $\Delta f$  of 0.05 MHz (broken lines) and 0.1 MHz (solid lines) above the critical frequency of the lower layer. There is a well-marked minimum close to the true valley depth (shown by the chain line) for both data sets. The two-parameter valley calculation, in which VDEPTH is adjusted to find the minimum value of DEVN, normally gives a good estimate of valley depth and an accurate profile for the upper layer. Poor results are obtained, however, if  $\Delta f = 0.1$  MHz and iteration begins from a too-large initial depth. The calculation can then settle at the spurious minimum near  $VDEPTH = 0.6$  MHz. Commencing iterations from a small value of VDEPTH does not cure this problem with all profiles. Two-parameter calculations in POLAN therefore begin by calculating the fit errors at the two values of VDEPTH shown by the dotted lines in Fig. 23. The depth giving the smaller value of DEVN is then chosen as the starting point for the iterative calculation. This procedure successfully finds the correct minimum, corresponding approximately to the correct valley depth, in all cases studied.

## 10. USING POLAN

### 10.1 Implementation

The subroutine POLAN uses 11 associated subprograms, as listed in Appendices F.2 to F.4. A short mainline program is also required to read the virtual-height data for each ionogram from a file, to call POLAN with appropriate parameters, and to store the resulting real-height data. All programs are written in FORTRAN, and conform to both the old FORTRAN IV (1966) and the new FORTRAN 77 standards. The complete set of programs will compile and run on a minicomputer with 56 kbytes (28 kwords on a PDP11) of RAM. These programs are available from the World Data Center-A; or from the author on IBM interchange format 8" diskettes or IBM PC-compatible 5 1/4" diskettes.

A simple mainline program POLRUN, for reading and processing prepared data files, is given in Appendix G.1. A more sophisticated program SCION for the scaling and analysis of ionograms is described in Section 11 and listed in Appendix F.5. This program accepts data from a digitiser, corrects for non-linearities and for skewed axes, and converts the result into frequency, height arrays. Ordinary and extraordinary ray data are then interleaved in the way required by POLAN, with ionospheric layers separated by a zero virtual height, and analysed. The scaled virtual-height data and the calculated real heights are written to output files.

When setting up a new ionogram analysis system, data can be scaled directly in the order used by POLAN. The general procedure will then be as outlined below. It is assumed that data entry uses a digitising table connected to a microcomputer or other programmable controller. Digitisation of "off-scale" areas, or direct keyboard entry, is used to set flags to show the nature of the data that follows. Flags are normally required to indicate "ORDINARY RAY DATA Follows"; "EXTRAORDINARY RAY DATA Follows"; "Scaled CRITICAL FREQUENCY"; and "END OF LAYER". Overall "End Of Data" is conveniently signalled by two successive "End Of Layer" flags.

Before scaling a set of ionograms, station identification is entered from the keyboard. This must include the latitude of the station, if the analysis is to calculate the value of START for a consistent model starting height (as outlined in Section 10.5). Alternatives to this calculation are (i) use of a fixed value of START for all ionograms (- a zero value will give the extrapolated starting height discussed in Section 6.2); or (ii) a separate value of start can be entered for each ionogram (in step (a1) below). The magnetic dip angle and the ground value of gyrofrequency are also entered at this stage. Steps (a) to (c) below are then followed for each ionogram.

(a)-- Preliminary.

(a1) Ionogram header data is entered from the keyboard. This must include the date and time of the ionogram if the mainline program is to calculate the value of START. Alternatively the value of START to be used for this ionogram can be entered at this stage. Determination of an appropriate value is discussed in Section 10.5.

(a2) Points are digitised to define the frequency and height scales. This will be similar to the procedure described in Section 11.3

(b)-- Starting the analysis.

(b1) Examine the low frequency section of the ionogram, identifying the lowest usable frequency ( $f_{min}$ ) for the O-ray. Sporadic-E traces are ignored. If the X-ray trace can not be identified at frequencies less than about  $f_{min}+1.0$  MHz, proceed to (b2) below. Set the flag for X-RAY DATA. Digitise X-ray points. The first point is at the lowest frequency possible. This is followed by about 4 further points at frequency intervals of about 0.1 MHz, giving a reasonable representation of the start of the X trace. There is no advantage in scaling X-ray points to higher frequencies; they will be ignored by POLAN. More detailed rules for data selection at this point are given in Section 10.4.3.

(b2) Set the flag for O-RAY DATA. Digitise points beginning (normally) at the lowest frequency  $f_{min}$ , and using a frequency interval of about 0.1 MHz. Spacing may be increased smoothly to 0.2 MHz or more at higher frequencies where the virtual heights are varying slowly. Where the virtual heights are increasing rapidly, near the peak of the layer, spacing may be reduced to about 0.05 Mhz with good data. Care must be taken to scale the frequency axis as accurately as possible near a layer peak (particularly if X-ray data will be used for calculating the size of the following valley).

When a gap occurs in an otherwise smooth section of the trace, there is no advantage in scaling points more closely at the ends of the missing region. POLAN will interpolate across the gap using several points from each side, and these points are best not concentrated in a small frequency range.

(c)-- End of a layer.

When a critical frequency can be identified by virtual heights which increase rapidly from below (near the peak of the lower layer) and from higher frequencies (reflected from the following layer), then an operator's estimate of the critical frequency is included in the analysis. This is particularly worthwhile when a vertical cursor can be adjusted to provide an approximate asymptote to virtual height traces at higher and lower frequencies. In this situation, flag "CRITICAL FREQUENCY" and digitise the estimated O-ray critical frequency FCO. If X-ray data also provide a good estimate of the critical frequency, flag "X-RAY DATA", flag "CRITICAL FREQUENCY" and scale the estimated X-ray frequency FCX. For scaled critical frequencies the controlling program inserts a zero value for the virtual height at the scaled frequency. X-ray points are indicated by making the scaled frequency negative in the normal way.

## 10.2 POLAN Input Data

### 10.2.1 Normal data

POLAN carries out the complete real-height analysis for one ionogram in response to the FORTRAN statement:

```
CALL POLAN (NDIM, FV, HT, FB, DIP, START, AMODE, VALLEY, LIST).
```

The first three parameters in this statement define the input virtual-height data, and (when POLAN returns) the calculated real-height profile. The next two parameters, FB and DIP, are required to specify the magnetic field constants. The remaining four parameters can be zero for most work, although for optimum results the parameter START should be used to specify a model starting height for the calculation. The meaning and use of the 9 parameters in the call to POLAN are described below.

(1) NDIM gives the maximum dimension of the data arrays FV, HT. This is set in the calling program so that the array dimensions may be varied to suit the amount of data being used and the size of the computer. Note that the number of data points given in these arrays must not exceed NDIM-32. NDIM must be given as a named variable (not just a number) since it is altered by POLAN to give the number of calculated real-height points returned after the analysis.

(2,3) FV and HT are arrays containing the frequency (f) and virtual-height (h') data to be analysed. Ordinary-ray data must be given in order of increasing frequency. This is checked by POLAN, to detect data errors. The end of the data for any one layer is indicated by a virtual height which is zero (or less than 30 km in absolute value; a non-zero value is used to modify the following valley calculation, as described in Section 7.4). The corresponding frequency - the critical frequency of the layer - is entered normally if it has been scaled; otherwise a frequency of 0.0 is given. If a valley is not wanted above an intermediate layer, the virtual height at the critical frequency is entered as 10.0; analysis of the next layer will then start from the height of the peak of the intermediate layer. (The same effect can be obtained by using a non-zero value for VALLEY, as described below.) The final end-of-data is signalled by two zero virtual heights. At the end of the analysis POLAN returns with frequencies and corresponding real heights in the arrays FV and HT; and NDIM gives the number of such data pairs.

Overall ordering of the input data in the arrays FV and HT is

```
          ( X START )          ( X VALLEY )
FV:      ( -F, . . . -F, ) F, . . . F, * 0, ( -F, . . . -F, ) F, . . . F, * 0, 0
HT:      ( -H, . . . -H, ) H, . . . H, 0, ( -H, . . . -H, ) H, . . . H, 0, 0
```

The sections in brackets are included only when extraordinary ray data are used for the start and valley calculations. The layer terminators, marked by \*, correspond to a point (0, 0) as shown when critical frequencies are not scaled. If a critical frequency is scaled the terminator becomes (FC, 0), where FC is positive for the O-ray and negative for the X-ray. If both O and X-ray critical frequencies are scaled there are two terminator points: (FC, 0) followed by (-FCX, 0).

(4) FB gives the gyrofrequency at the ground in MHz. The program then assumes an inverse cube variation with height corresponding to the relation

$$FH = FB.(1 + h/6371.2)^{-3}.$$

To use a constant value of gyrofrequency in the analysis, FB is set equal to minus the desired value (as in Section 10.2.2).

(5) DIP gives the magnetic dip angle in degrees. The same value is used at all heights.

(6) START is used by POLAN to define the starting height, for an O-ray analysis. The real-height calculations normally begin from a starting frequency  $f_s$  of about 0.5 MHz. If START = 0, POLAN derives a starting height  $h_s$  to use at this frequency, by extrapolating the first few virtual height data points and limiting the result to a reasonable range. It is normally preferable to enter a model value for the starting height; this is done by setting START =  $h_s$  where  $h_s$  must be greater than 44 km. The given value is reduced if necessary to be compatible with the initial virtual-height data. Procedures for determining a suitable value of START are described in Section 10.5 below.

For a combined O and X-ray start calculation, START is used to give the mean height at which to calculate the gyrofrequency for the underlying region. This mean height has been found to be very close to the optimum starting height for an O-ray calculation (Appendix C.5), so that the normal model values of START are still appropriate. Start calculations using X-ray data also incorporate any model value of START in the least-squares solution, with a low effective weight, so that indeterminate data will not give unreasonable results. Thus for all calculations, with or without X ray data, best results will normally be obtained by specifying a value of START determined as in Section 10.5.

(7) AMODE specifies the type of analysis, and may be zero for all routine calculations. POLAN then uses the mode 5 analysis (changing to mode 15 at high dip angles) which appears most suitable for general work. This default setting can be changed by altering the two lines "IF (MODE.EQ.0 . . ." in section C1.1 of POLAN. Other possibilities, ranging from a linear lamination analysis to a single-polynomial calculation (using a single analytic expression for each layer) are obtained by setting AMODE equal to some value from 1 to 9, as described in Section 5.2. If maximum numerical accuracy is required the normal 5-point integrals must be replaced by 12-point integrals; this is achieved by adding 10 to AMODE, giving a value in the range 11 to 19.

(8) VALLEY should be zero for most routine calculations. POLAN then inserts between layers a valley selected from the "standard" family shown in Fig. 17. The width (in km) and depth (in MHz) of this valley depend on the height of the underlying peak, and will normally be close to the values given in Table 5 of Section 7. To omit valleys altogether, giving a monotonic profile, set VALLEY = 10.0. The result gives a lower limit to the range of possible profiles for the upper layer. An upper limit, corresponding approximately to the maximum feasible valley width, is obtained by setting VALLEY = 5.0. Other variations to the standard valley shape are summarised in (8) below. Note that the value of VALLEY can be overridden for a particular ionogram by inserting a non-zero virtual height at the final data point for the previous layer, as described in Section 7.4.

(9) LIST is zero to produce the normal summary listing during the run of POLAN. This includes information relating to an extraordinary ray start calculation, a valley calculation, and the parameters at a layer peak (Section 10.3.2). Data errors also produce a printed line. Other values of LIST suppress the output or give more detail of the analysis steps, as described in (9) below.

#### 10.2.2 Further options (ignore these until you are familiar with the program)

Any of the input parameters in the call to POLAN (other than NDIM) can be made negative, or modified in some other way. This signals some departure from the standard analysis procedure, as described below. Many other features of the calculations can also be changed. Interested workers should study the appropriate sections of this report and the program listings.

(1) NDIM is not modified. It must always be a "variable" giving the maximum dimensions of the data arrays FV, HT as set in the calling program. The number of data points must be less than NDIM-32.

(2) FV: Negative frequencies are used to denote extraordinary-ray data. Such points immediately precede the ordinary ray data for each layer, in the arrays FV and HT. Within each set of X-ray data, the absolute values of frequency should increase monotonically; this is used by POLAN as a check on data integrity.

(3) HT: A negative virtual height  $h'_i$  is used to allow a gradient discontinuity in the  $N(h)$  profile. Heights will be calculated up to the corresponding frequency  $f_i$ , using a virtual height  $|h'_i|$  at this frequency. Calculations then continue with a new polynomial beginning from the calculated real height  $h_i$  at the frequency  $f_i$ . The result has a discontinuity in the gradient  $dh/dFN$ , and in all higher derivatives, at  $f_i$ . This procedure has been recommended for use with parabolic lamination calculations (e.g. Wright, 1967). It is not normally required with higher order modes of analysis, in which points of inflection can occur between scaled frequencies, and tests show that with all methods it is generally better not to scale the cusp (Section 10.4.1; and Titheridge, 1982).

(4) FB: A negative value of the gyrofrequency FB gives an analysis in which the gyrofrequency is assumed to be independent of height. This is useful mainly for carrying out tests using model ionograms which have been calculated assuming a constant gyrofrequency. The value of FB should apply to a height of about 150-200 km for night-time ionograms, or about 100 km if X-ray data are being used for an E-layer start calculation.

(5) DIP: Calculated starting and valley corrections using extraordinary-ray data are normally subject to physical constraints, discussed in Sections 8.4 and 7.3. The initial gradient  $dh/dFN$  of the polynomial section must be positive, the width of the valley or the starting height correction must be positive, and in the slab start the thickness of the underlying slab of ionisation must be positive. These restrictions can be omitted by setting DIP negative.

(6) START: Corrections for underlying ionisation can be suppressed by setting  $START = -1.0$ . Analysis of O-ray data then begins from the first scaled frequency  $f_1$ , with a real height equal to the least of the first three virtual heights. Calculation of a starting correction using extraordinary-ray data, whenever this is given, is not affected. Values of  $START$  less than  $-1.0$  cause X-ray calculations to use the polynomial start procedure of Section 8.6.1.  $START$  can be set equal to minus the model O-ray starting height, to give the normal model start with O-ray data and a polynomial start when X-ray data are provided. Values of  $START$  in the range  $-1.1$  to  $-3.0$  cause the polynomial start to begin at a frequency of  $-START-1$  MHz. Note that the polynomial start gives increased flexibility in the unseen region, when  $f_{min}$  is large, and so tends to give more variable results. The uses of  $START$  are described more fully in Sections 6.2 (for O-ray data) and 8.6 (for X-ray data).

(7) AMODE: Starting and valley calculations using combined O- and X-ray data normally incorporate several physically-desirable conditions in the least-squares solution (Sections 8.4 and 7.3). These conditions are omitted if the value of AMODE is negative. The calculated profile will then be a better fit to the virtual-height data, but (with medium or poor quality data) may be a less reasonable result on physical grounds. Thus to obtain the unrestricted best-fitting profile, using the normal (default) mode of analysis, set DIP negative and  $AMODE = -5$ .

(8) VALLEY: With ordinary ray data, the parameter VALLEY can be used to adjust the size of the valley inserted above a layer peak. To increase or decrease the width of the valley, set the parameter VALLEY equal to the required scaling factor (which must be in the range 0.1 to 5.0). If the resulting valley width is unrealistically large, it will produce a small or negative value for the real-height gradient  $dh/dFN$  just above the valley; the width of the valley is then automatically reduced, to give a gradient equal to the local scale height (Section 7.3.3). In all cases (when VALLEY is not negative) the depth of the valley is varied as the width changes, so that the final valley represents a selection from the family of "standard" valleys shown in Fig. 17. Specific values of width and/or depth can also be set for the valley region by using negative values for VALLEY, as described in Section 7.4.

With extraordinary ray data the one-parameter valley calculation is recommended for general use. This is the default procedure obtained when  $VALLEY = 0.0$  or  $1.0$ . It selects the best-fitting valley from the family shown in Fig. 17, by determining the width that gives the smallest RMS deviation between the given virtual height data and virtual heights corresponding to the calculated profile. For detailed studies using high quality data, when it is desired to obtain the maximum possible amount of information from an ionogram (and in particular when it is suspected that a wide but abnormally shallow valley may be present) the two-parameter analysis can be used (with caution). This is obtained by setting  $VALLEY = -1$ . The width and depth of the valley are then determined separately. Results obtained give a reduced RMS deviation between the given virtual height data and those corresponding to the calculated real height profile. However, since the data are never exact, the calculated profile is not necessarily better than the normal one-parameter result.

(9) LIST: If  $LIST = -1$  all direct printed output from POLAN is suppressed. At  $LIST = 1$  the subroutine TRACE is called to list the real-height constants at each step. Larger values of LIST (up to  $LIST = 5$ ) produce fuller trace output for debugging purposes. Adding 10 to the value of LIST restricts the added trace outputs to the start and valley calculations.

### 10.3 POLAN Output Data

#### 10.3.1 Data returned within the program.

The subroutine POLAN is called with frequency and virtual height data in the arrays FV and HT. It returns with frequencies and corresponding real heights in these arrays. The returned frequencies will differ from the given data frequencies since extraordinary-ray points have been deleted, and additional real-height points have been added to define better the start, valley and final peak sections of the profile.

For an O-ray start, the real-height profile begins with a polynomial section from a frequency which is normally 0.5 MHz, but is constrained to lie in the range  $0.35f_{min}$  to  $0.6f_{min}$ , (where  $f_{min}$  is the lowest scaled frequency). A further point is added at a frequency of  $0.6f_{min}+0.2$  MHz. With an X-ray start, the low-density ionisation is represented by a linear-in-FN lamination from  $0.3f_{min}$  to  $0.6f_{min}$ . The polynomial real-height profile starts at  $0.6f_{min}$ , and a further point is added at  $0.8f_{min}$  to define this adequately. Heights given at plasma frequencies less than  $f_{min}$  should not be taken as a true representation of the profile shape. They serve only to give approximately correct values for the total amount of underlying ionisation and for the ionisation gradient near  $f_{min}$ .

In each valley region, above a layer peak, four additional points are inserted. The first two are at plasma frequencies of  $FC-V/2$  and  $FC-V$ , where  $V$  is the valley depth. These points define a parabolic continuation of the layer peak, with a scale height of  $1.4 SH$ . The next point, also at  $FN = FC-V$ , shows the extent of the flat valley-bottom region (illustrated in Fig. 6). Finally a point at  $FN = FC$  defines the top of the valley, and the start of the next layer. The shape of the valley and the ratio of depth to width are essentially defined by models (since these quantities can be determined directly only by careful analysis of unusually good O and X data). For O-ray calculations the valley width is also basically a model value, dependent on the mean neutral scale height, the value of  $SH$  for the underlying peak, and the gradient and curvature at the base of the next layer. When X-ray data are used in a valley calculation the width is a directly calculated parameter, biased to a varying extent by the models so that an ill-defined calculation will not yield absurd results (Section 8.4).

Three points are added after the peak of the final layer, at distances of 0.5, 1.0 and 1.5 scale heights above the peak. These give an exact Chapman-layer extrapolation of the calculated peak, assuming a typical scale height gradient  $dSH/dh$  of 0.1. They show the initial variation in the topside ionosphere, and simplify the averaging of profiles with different peak heights.

POLAN returns with the first subroutine parameter (NDIM) altered to a value  $N$  which gives the array position of the last profile point. Thus the last calculated real-height point is  $HT(N)$ ,  $FV(N)$ . Other information is returned in the following two elements of the arrays:

$FV(N+1)$  = twice the standard error in the calculated critical frequency.

$HT(N+1)$  = twice the standard error in the calculated peak height  $HMAX$ .

$FV(N+2)$  = the total electron content of the calculated profile up to the height  $HMAX$ . This is obtained by exact integration of the individual polynomial real-height expressions, and is given in units of  $10^{10}$  electrons/m<sup>2</sup>.

$HT(N+2)$  = the calculated scale height  $SH$  for the peak of the final layer.

$FV(N+3) = HT(N+3) = 0.0$  to terminate the output data.

Note that these errors indicate only the accuracy of the least-squares peak fit. Consistent data errors near the peak can lead to incorrect peak parameters with a small standard error. The error in  $HMAX$  also does not include the effect of real-height errors produced at lower frequencies (from incorrect values for the start and valley regions, for example).

#### 10.3.2 Printed outputs from POLAN

If the input parameter LIST is negative, POLAN produces no printed output and the only results available are those returned through the calling parameters and described in Section 10.3.1. In a normal calculation with  $LIST = 0$ , four types of printed output occur.

(i) If there is a data error, detected as an incorrect sequence of ordinary-ray frequencies in the array FV, the program prints:

The two successive frequencies listed are in an incorrect relation. For X-ray data, denoted by negative frequencies, an error is detected if a value of  $|f|$  is less than that for the first X-ray point for the layer considered. When a data error is found POLAN returns with all previously calculated (and presumably correct) real-height data in the arrays FV(I) and HT(I), where I = 1 to N. That these data do not correspond to a complete analysis is indicated by a zero value for SH in HT(N+2). The printed output shows the above error message, and no peak listing.

(ii) If extraordinary-ray data are given at the start of the analysis, the constants involved in the start calculation are listed in a line of the following form, where bracketed values represent numerical data.

(NC) start offset = (A) km, slab (B) km. devn (D) km  
(NT) terms fitting (NO) 0 + (NX) X rays + (NP). hx = (FHHT).

(NC) gives the number of iteration cycles required in the calculation. This is normally 1 when the gyrofrequency is constant with height, and 2 or 3 if it is varying.

(A) gives the amount by which the calculated starting height for the first polynomial is less than the initial value obtained from a limited extrapolation of the ordinary-ray virtual heights. A zero value of A indicates that the calculations originally gave a negative value, which was set equal to zero.

(B) is the thickness of the underlying slab of ionisation (from  $FN = 0.3f_1$  to  $FN = 0.6f_1$ ). This is zero if the data initially gave a negative value or if a polynomial start is being used.

(D) is the RMS deviation between the given virtual height data and virtual heights calculated from the final real height curve. D gives approximately the error with which the ordinary-ray virtual heights are fitted. For extraordinary-ray data the mean error is about 2D, because of the reduced weight given to X-ray data in the least-squares solution.

(NT), (NO) and (NX) give the number of variables determined in the starting calculation, and the number of ordinary and extraordinary-ray data points used in the calculation. (NP) is the number of equations representing physical constraints. Thus the total number of equations included in the solution is  $NO + NX + NP$ ; if this is greater than NT then a least-squares calculation has been used.

(FHHT) is the calculated height of reflection of the first or second extraordinary-ray frequency. This is the height used to calculate the value of gyrofrequency to use in the analysis. Calculations using X-ray data and a height-varying gyrofrequency are iterated until FHHT changes by less than 2 km.

(iii) For each layer peak a line is printed giving the critical frequency at the peak in MHz; the peak height in km; the calculated scale height (printed negative if an unreasonable value was replaced by a model value); and the slab thickness (equal to the total electron content divided by the peak density) in km. Some error indications are also given for the peak parameters; these are as described in Section 10.3.1.

(iv) A valley is inserted between successive layers (unless 0-ray data only are provided, and a zero valley is specified by using VALLEY = 10.0). At each valley calculation the following line is printed.

(NC) VALLEY (W) KM WIDE, (V) MHz DEEP. DEVN (D) km.  
(NT) TERMS FITTING (NO) 0 + (NX) X RAYS + (NP). HX = (FHHT).

(NC) is the number of iteration cycles used in the analysis; this exceeds 2 only for X-trace calculations. (W) is the distance from the peak of the underlying layer to the point with the same density in the upper layer. (V) represents roughly the mean decrease of plasma density in the valley. (D) is the RMS virtual-height fitting error in the valley calculation. POLAN has fitted an expression with (NT) variables to a set of  $NO + NX + NP$  simultaneous equations, making use of (NO) scaled 0-ray data points, (NX) X-ray points, and (NP) physical constraints. The latter represent semi-empirical relations between the size and shape of the valley, the neutral scale height, the plasma scale height SH, and the gradient at the base of the following layer.

(FHHT) gives the height of reflection of the first or second extraordinary ray used in the analysis, or the first ordinary ray if there are no X-ray data. For X-ray calculations with a height varying gyrofrequency, each step in the valley analysis is iterated until FHHT changes by less than 2 km.



An extraordinary-ray valley analysis always produces several listed lines. For a one-parameter analysis there are normally three lines. These correspond to the initial valley depth  $V$ , and two subsequent corrections in which  $V$  is scaled approximately as  $W^2$  (Section 7.2). If the RMS deviation  $D$  increases too much on the third iteration the previous calculation is repeated, giving a fourth printed line which is identical to the second. For a two-parameter valley analysis the first two lines are the same as for the one-parameter analysis. Thereafter further lines are listed corresponding to changes by a factor of about 1.4 in the assumed depth, until a minimum of  $D$  is found. A final line using the depth  $V$  interpolated for minimum deviation is then obtained.

## 10.4 Selection and Scaling of Data

### 10.4.1 General considerations

The amount of data which need be scaled from an ionogram, to obtain near-optimum accuracy in the calculated real heights, depends primarily on the ionogram. Thus the rules outlined here for data selection are applicable to most methods of analysis. Polynomial methods are however somewhat less dependent on the choice of data, compared with lamination methods, since they can interpolate a point of inflection between scaled frequencies.

The effects of using different frequency intervals  $Df$  with ordinary (O-)ray data have been studied elsewhere (Titheridge, 1982). Smaller values of  $Df$  are required where the virtual heights are changing most rapidly, as near the F1-layer cusp in Fig. 24. If the scaling interval is too large we get a fluctuating error in the cusp region, and an overall error at higher frequencies. These errors are approximately the same for all methods of analysis. With a typical cusp, real-height errors at and above the cusp begin to decrease at  $Df \approx 0.15$  MHz for polynomial calculations, and at  $Df \approx 0.09$  using parabolic laminations. Errors are typically about 1.2 km at  $Df = 0.2$  MHz, 0.5 km at  $Df = 0.1$ , and 0.1 km at  $Df = 0.05$  MHz (using the default mode of POLAN). Thus a frequency interval of about 0.1 MHz is normally adequate.

POLAN will allow the real-height gradient to be discontinuous at a cusp, if  $h'$  is made negative at the cusp frequency (Section 10.2.2). Tests show, however, that this increases the real-height errors with all methods of analysis (Titheridge, 1982). Best overall results are obtained with model ionograms when the cusp lies approximately midway between scaled frequencies, as shown in Fig. 24. This will also be the best procedure with practical ionograms since the virtual height at the cusp is not a stable and accurately measureable quantity.

The careful selection of data points is most important for calculations involving the "unseen" regions in the ionosphere. These are the underlying or start region where the plasma frequency  $FN$  is less than the minimum observed frequency  $f_{min}$ , and the valley region between ionospheric layers where  $FN$  is less than the critical frequency  $FC$  of the underlying peak. For an accurate real-height profile we must determine the extent of these regions using combined ordinary and extraordinary ray measurements. The choice of scaling frequencies for start and valley calculations is investigated in Sections 8.5 and 9.4. Some checks are carried out within POLAN, as described in Section 8.2.3, to eliminate unhelpful or possibly harmful data from the start and valley calculations.

Sporadic traces should not be digitised. These traces are characterised by a sharp cusp (generally in the E layer), a short rapid decrease in  $h'$ , and a flat section of varying length with no significant increase in  $h'$  at the high frequency end. They are produced by thin, near-horizontal ledges superposed on the main  $N(h)$  profile. If the main E-layer trace can also be seen (i.e. the sporadic layer is transparent) this main layer should be scaled. More commonly the sporadic layer blocks out a section of the true E layer trace. There will then be a gap in the series of scaled points, as shown in Fig. 24. Do not scale additional points at the ends of the gap. The overlapping polynomial procedure in POLAN will provide a smooth interpolation across the gap, and this interpolation is preferably not restricted to points over a narrow frequency range at each end. Typical scaling points for an ionogram which includes short sporadic-E traces are shown in Fig. 24.

### 10.4.2 Selection of ordinary ray data

Ionogram scaling normally begins at the lowest observed O-ray frequency  $f_{min}$ . The first few points are scaled at a frequency interval of about 0.1 MHz, so that the first 5 points cover a frequency range of about 0.4 MHz. This is particularly important when X-ray are to be used in the start calculation. At least 4 points should be scaled before retardation caused by the following layer peak becomes large; this will occasionally require the use of an initial frequency spacing less than 0.1 MHz. When the trace is irregular or ill-defined at low frequencies, additional points may be scaled in the range from  $f_{min}$  to  $f_{min}+0.4$  MHz. POLAN includes such points in a start calculation automatically, with most modes of analysis (Section 8.2.3).

After the first 5 points, the scaling interval may be increased to 0.2 MHz or more in regions where the virtual height is changing slowly. Near critical frequencies or sharp cusps the frequency interval is decreased so that the height changes are less than about 10 km between successive points. A minimum practical or worthwhile frequency interval is about 0.05 MHz. Abrupt changes in Df should be avoided (so that calculation of a real-height segment is not unduly weighted by data at one end of the segment).

In some night-time ionograms the virtual heights increase rapidly towards  $f_{min}$ . Decreased values of Df should not be used in this region in an attempt to obtain greater accuracy by defining the changes in  $h'$  more closely. If the initial changes in  $h'$  exceed about 20 km in an interval of 0.05 MHz, this part of the trace should be ignored. This is because a rapid increase in  $h'$  at low frequencies indicates retardation due to a dense underlying peak, which can not be allowed for accurately (Section 8.5.2). Thus the circled section of the trace in Fig. 25(a) is not scaled.

Digitizing continues up to the critical frequency defining the end of the first layer. Critical frequencies show as a rapid increase in  $h'$ , tending to a vertical asymptote, followed by a break in the recorded trace. This is shown at foE and foF2 in Fig 24. If the position of the critical frequency can be judged with reasonable accuracy, using the increase in group heights for both the first and second layers, it should be scaled (at any convenient height). The E-layer trace in Fig. 24 does not provide a good indication of the position of the critical frequency, so scaling of foE is not desirable. If the F1-layer trace extended to lower frequencies, as shown by the dotted line, an estimated value of foE should be scaled. Scaled critical frequencies are not taken as exact but provide additional input to the least-squares peak calculation.

The second (F-layer) trace is digitised from just above foE up to the next critical frequency. This is normally foF2, although there may occasionally be a true discontinuity, and a critical frequency, at foF1. Any part of the F-layer trace between foE and foE+0.1 MHz, or with  $dh'/df < -200$  km/MHz, should be ignored (as shown in Fig. 25b). This is because the virtual heights in this region depend more on the detailed shape of the E-layer peak than on the F-region heights; they are also more affected by horizontal gradients in the ionosphere. The first 5 or 6 F-layer points should cover a range of about 0.4 to 0.7 MHz, particularly if these data are to be used with corresponding X-ray data in a O/X valley calculation.

#### 10.4.3 Selection of X-ray data, for start and valley calculations

X-ray data are used only when there is some important piece of information which cannot be obtained without them. Scaled X-ray data are therefore of three types:

- (a) for start calculations, X traces which continue down to frequencies within about 1.0 MHz of the lowest observed O-ray frequency;
- (b) for valley calculations, any X traces which show group retardation due to the underlying peak (so that virtual heights increase at the low frequency end of the trace);
- (c) traces which give a useful measure of the critical frequency FCX of a layer peak. These provide additional input for the least-squares peak calculation in POLAN.

The frequencies used in start and valley calculations should be those at which the virtual heights depend primarily on the unseen ionisation (as discussed in Appendix B.2) and are not dominated by other effects. Thus, for example, valley calculations should not include measurements too close to the critical frequency of the underlying peak. Data at frequencies well above the region of interest are also best omitted. The difference  $h'_x - h'_o$  due to underlying ionisation decreases rapidly with increasing frequency, so use of a frequency range greater than about 0.7 MHz adds little information and may include unwanted variations in the gradient at reflection (Section 8.5.2). These basic considerations apply to all methods of real-height analysis.

If there is a suitable E-layer X-ray trace present for daytime ionograms, or a suitable F-layer X-ray trace present for night-time ionograms, a joint O-X solution may be found for the starting height. This is a rare event for daytime ionograms, but quite common for night-time ionograms. For good results, corresponding O and X rays should be reflected at approximately the same values of plasma frequency FN. That is, the O-ray frequencies  $f_o$  and the X-ray frequencies  $f_x$  should correspond approximately to the relation

$$f_o^2 = f_x \cdot (f_x - FH) \quad (32)$$

where FH is the gyrofrequency at the appropriate height (usually about 200 km at night). A table of corresponding values of fo and fx should be prepared as an aid to the selection of X-ray data.

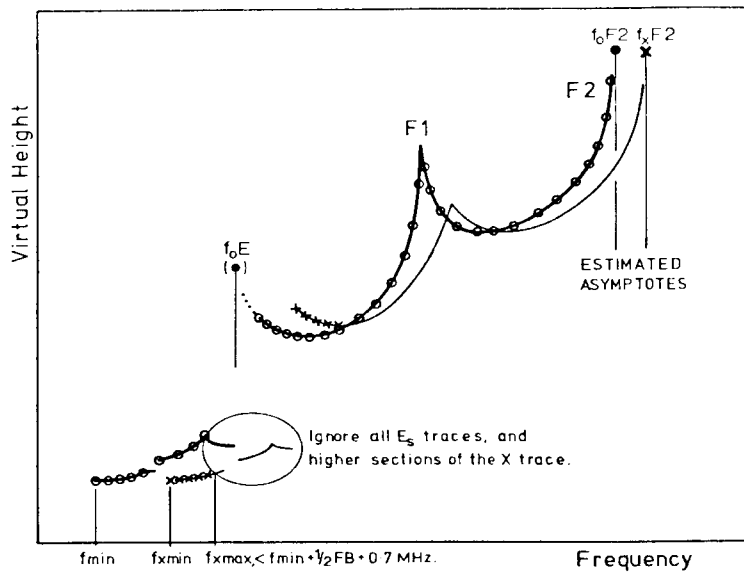


**Figure 24.** A representative daytime ionogram showing E and F2 layers, and an F1 cusp. Thick and thin lines give the ordinary and extraordinary ray traces respectively. Corresponding scaled points are shown as o or x. Solid symbols are for scaled critical frequencies.

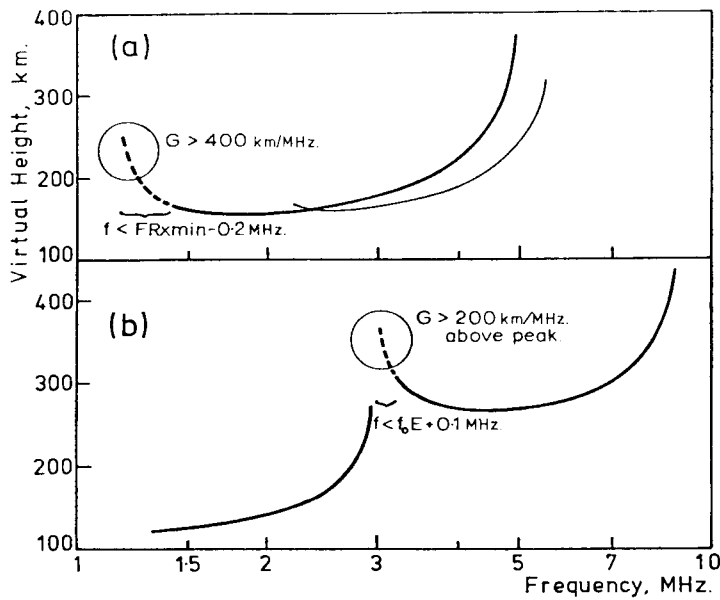


**Figure 25.** Night-time (a) and daytime (b) ionograms showing, as broken lines, the parts of the ordinary ray trace which should not be scaled.  $G$  is the absolute virtual-height gradient  $|dh'/df|$  in km/MHz.

If  $f_{min}$ ,  $f_{xmin}$  are the lowest usable frequencies for the O, X traces respectively, and  $FB$  is the ground value of the gyrofrequency, we require (ideally) that  $f_{xmin} \approx f_{min} + 0.5FB$ . In practice O/X analysis is generally worthwhile if the X-ray trace is recorded down to a frequency  $f_{xmin}$  such that

$$f_{xmin} < f_{min} + 0.5FB + 0.5 \text{ MHz.} \quad (33)$$

It is occasionally helpful to omit some initial O-ray data, increasing the value of  $f_{min}$  so that (33) holds. This should be done only when it leaves sufficient, accurate data for both O and X traces, without including any points affected by peak retardation. In the example of Fig. 25(a), the X-ray trace extends down to a frequency  $f_{xmin}$  of 2.2 MHz. This corresponds to a plasma frequency at reflection ( $FR_x$ ) of 1.62 MHz, at  $FH = 1.0$ . The X-ray trace is showing retardation from the underlying ionisation, so an X-ray start is definitely worthwhile. The marked section of the O-ray trace, at  $f < 1.42$  MHz, should not be scaled.

Five to eight points are scaled at the start of the X trace. These points should be at frequency intervals of about 0.1 to 0.05 MHz, covering a frequency range of about 0.5 MHz (Section 8.5). The maximum useful X-ray frequency for start calculations is

$$f_{xmax} < f_{min} + FB + 0.6 \text{ MHz.} \quad (34)$$

X-ray data at wave frequencies higher than  $f_{xmax}$  are deemed 'not-useful' by POLAN, and will be omitted from the analysis.

X-ray data which are showing the effects of retardation in a following peak will be ignored by POLAN, and need not be scaled. As frequencies increase towards a layer peak, the virtual heights begin to increase rapidly. The group retardation of the O and X rays is then more dependent on the characteristics of the peak than on the underlying ionisation, and is not useful for starting calculations. POLAN normally ignores X data for which  $dh'/dfx$  exceeds +40 km/MHz. When there is only a short frequency range between  $f_{min}$  and the first critical frequency, it may be necessary to use smaller values of  $Df$  so that 5 points can be scaled before peak retardation becomes important (Section 8.2.3).

Very large virtual heights, at frequencies less than 0.1 MHz above a critical frequency, should not be scaled. Any such points are ignored by POLAN, since the virtual heights depend more on the precise density and thickness of the E layer peak than on the size of the E-F valley. These highly retarded rays also have larger horizontal deviations, and so are more likely to be affected by the presence of horizontal gradients in the ionosphere.

The use of extraordinary-ray data by POLAN is discussed more fully in Sections 8 and 9, and in Appendix B.2. Scaling rules are most important with difficult ionograms, and are designed for maximum reliability, consistency and accuracy under difficult conditions. Suitable rules for selection of start and valley data, incorporating the above considerations, are given below.

- (i) Virtual height traces with  $|dh'/df| > 200$  km/MHz are ignored in start and valley calculations (Section 8.5.2). With this proviso, scalings commence from the lowest observed frequencies.
- (ii) About 5 X-ray points are scaled, using a frequency interval  $Df > 0.05$  MHz. X-ray data then cover a range of at least 0.2 MHz, to give a reasonable measure of the changes in  $h'_x - h'_o$ .
- (iii) For both O and X rays we use frequency intervals  $Df < 0.2$  MHz, giving a maximum range of about 0.8 MHz for the 5 points (for each component) used in a start or valley calculation.
- (iv) Scalings should not extend up to frequencies where there is appreciable retardation due to a cusp or peak. In some cases this will require use of a smaller value of  $Df$ , to obtain 5 points for a start calculation.
- (v) If  $FR_{xmin}$  is the plasma frequency at reflection of the first scaled X ray, O rays should not be scaled at frequencies less than about  $FR_{xmin} - 0.2$  MHz. Thus if  $f_{xmin}$  is the lowest usable X-ray frequency, O-rays are not scaled at frequencies below about  $f_{xmin} - 0.8$  MHz.
- (vi) If X traces are observed to plasma frequencies  $FR_x$  lower than the minimum O-ray frequency  $f_{min}$ , they may be scaled down to a plasma frequency of about  $f_{min} - 0.4$  MHz corresponding to a wave frequency of about  $f_{min} + 0.3$  MHz. This is subject to condition (i) above.

The reasons for (v) are the same as those incorporated in (iii). Information about the unseen ionisation is contained primarily in the quantity  $h'_x - h'_o$ , for O and X rays reflected near the same real height. Inclusion of lower O rays only, adds little information about the unseen region but increases the range (and hence the possible complexity) of the reflecting region used in the start calculation. (vi) allows a larger range of acceptance for X-ray data, without corresponding O rays, since the X rays are more affected by retardation in the unseen region.

For routine use, the above rules may be shortened to:

- (a) Ignore low-frequency traces which are curling up with a gradient greater than 200 km/MHz.
- (b) Ignore X traces showing retardation in a following peak.
- (c) The lowest scaled frequencies  $f_{min}$  (O-ray) and  $f_{xmin}$  (X-ray) should be such that
$$f_{min} + 0.3 < f_{xmin} < f_{min} + 0.8 \text{ MHz.}$$
- (d) Scale O and X traces at a frequency interval of about 0.1 MHz.

### 10.5 Selection of a Value for START

When extraordinary ray data are available to calculate a starting correction, the value of START given in the call to POLAN (or calculated within POLAN, if the given value is zero) is used only to define a suitable mean height at which to calculate the gyrofrequency for the underlying ionisation. The normal O-ray values of START are quite appropriate for this purpose (Appendix C.5), so use of X-ray data requires no change in the input parameters to POLAN. The normal X-ray starting model consists of a linear slab or lamination covering a range of plasma frequencies from  $0.3f_{min}$  to  $0.6f_{min}$ , where  $f_{min}$  is the lowest plasma frequency at which a virtual height (O-ray or X-ray) is given. The first real-height polynomial then begins at  $0.6f_{min}$  (Section 8.3). If the parameter START is negative we get the alternative start correction consisting of a single real-height polynomial from a frequency of 0.5 MHz (or  $0.8f_{min}$  if this is less than 0.5 MHz; Section 8.6). This gives added flexibility in the start region when  $f_{min}$  is large, and so tends to give more variable results.

Ordinary ray calculations begin with a real-height polynomial from a starting frequency  $f_s$  which is less than the lowest data frequency  $f_{min}$ .  $f_s$  is nominally 0.5 MHz, but is kept within the range  $0.35f_{min}$  to  $0.6f_{min}$ . When  $START = 0$ , POLAN obtains a starting height  $h_s$  by a bounded extrapolation of the first few virtual-height points, as described in Section 6.2(a). If no starting correction is desired, use  $START = -1.0$ . The real-height calculations then begin directly from the first scaled frequency, with a height equal to the lowest of the first three virtual heights.

Inadequate starting data is a common difficulty, and the main source of error in analysis of the daytime E layer and the night-time F layer. For maximum accuracy and reliability a model value of START should be used to define a suitable starting height  $h_s$ . The optimum value depends on local time, season and (to a lesser extent) on the latitude of the recording site. Suggested model values, derived from an analysis of published D region and night-time E region profiles, are described in Sections 6.3 and 6.4. For daytime conditions, when a normal E-layer trace is present, Table 4 is used to obtain a suitable, consistent model value for START. At night, when there is no E-layer trace, the value of START is obtained from Fig. 4. If the E-layer trace can be scaled, near sunrise and sunset, START is set equal to about 90 km (as shown by the thin lines in Fig. 4).

For some purposes an approximate mean starting correction is adequate. The following values of START, based on the results of Sections 6.3 and 6.4, can be used for stations at all latitudes and at all seasons.

START = 80 km	within a few hours of local noon.
START = 88 km	about 2 hr after sunrise, or 2 hr before sunset, when an E-layer trace is still present.
START = 90 km	near sunset and sunrise, when the E-layer trace is still observed.
START = 80 km	near sunset and sunrise when data begins in the F-region.
START = 100 km	at 1 hr after local sunset.
START = 130 km	at 2 hr after local sunset.
START = 150 km	from 4 hr after sunset to 1 hr before sunrise.

When only ordinary ray data are available, these entered values for START provide a model starting height  $h_s$  which gives a consistent, mean allowance for the effects of low-density ionisation. When combined O and X ray data are used to calculate an improved starting correction, the same values of START provide a suitable mean height at which to calculate the gyrofrequency for the underlying ionisation (Appendix C.5).

When many ionograms are being analysed from one station, tables are prepared (from the data in Sections 6.3 and 6.4) giving the value of START as a function of season and local time. For more general use an approximation to these values of START can be calculated for each ionogram, within the analysis program. This requires that the station latitude, and the date and local time of each ionogram, have been entered as outlined in Section 10.1. The solar zenith angle  $\chi$  is then calculated from the equation in Section 6.3(b). When  $\chi$  is less than  $95^\circ$ , and virtual heights are recorded from the E layer, START is set equal to the value of  $h_{0.5}$  calculated from equation 10 of Section 6.3. At night, when an E layer trace can not be scaled, the value of  $\chi$  is used to obtain a suitable value of  $h_s$  by numerical interpolation in the results of Figure 4.

## 11. SCALING AND ANALYSIS WITH THE PROGRAM SCION

### 11.1 Outline

In this section the practical use of POLAN is illustrated in terms of a specific implementation, using a programmable digitizer. The programs involved were developed originally by McNamara (1978, unpublished) for use at the WDC-A, Boulder. A similar system at the Ionospheric Prediction Service (Sydney), using a Summagraphics Bit Pad and an LS111/03 computer, is described by McNamara (1982). All calculations use the standard or 'default' options in POLAN. The scaling procedure described here offers an alternative to the system outlined in Section 10.1, in which data are scaled directly in the order required by POLAN.

The complete analysis involves three stages:

- (a) Digitize the ionogram, using a scaling table, to create a computer file with frequency, height data points in arbitrary units. This process will vary with the type of scaling table used. The digitised data are read line by line by the program SCION, and must be in the form detailed below and in the listing of SCION (Appendix F.5). Typical steps involved in the digitizing process are described in Sections 11.2 to 11.4 below.
- (b) Correct the data points for non-linearities in the ionogram, convert them into actual frequencies and heights, and combine ordinary and extraordinary ray measurements into the form required by POLAN.
- (c) Run POLAN to obtain the required  $N(h)$  profile.

The digitizing procedure in step (a) was developed for use with a Hewlett Packard 9864A digitizer and digitizing table. An appropriate program was written for the associated HP 9821A calculator by McNamara. Descriptive headings (Section 11.2), coordinates (Section 11.3) and data points (Section 11.3) are entered into a file which we shall call NHDATA. At the end of each logical step in the digitizing process, identified by the digitizing of an "off-scale" point, the display flashes and a prompt message appears to indicate the next step.

Data points are recorded as 6 pairs of (frequency, height) coordinates per line of file. After 6 points, the system is inactive while a carriage return is executed. Do not digitize during this period. After the carriage return, the current prompt is repeated. When the complete ionogram has been digitized the entry (or TEXT) mode of the digitizer is terminated by control/C. The file is then packed (with the instruction PACK) and saved (by SAVE NHDATA). The resulting file NHDATA provides all input data for the program SCION. NHDATA may be edited as required, to alter the header data or to correct or delete scaled points, if the initial run with SCION appears unsatisfactory.

Step (b) above is performed by the program SCION, which takes its input data from the file NHDATA (on unit 6). Correction of the data points is carried out using the subroutines DESKEW and INTERP. DESKEW corrects all data pairs for departures of the ionogram axes from a rectangle parallel to the axes of the scaling table. INTERP converts the scaled and deskewed positions into frequencies and heights; this is done by 4-point polynomial interpolation in scaled frequency and height marker positions. Finally SCION combines the O- and X-ray data into the form required by POLAN (Section 10.2). The data points are printed by SCION, before and after correction, to provide a check on the overall scaling process. Listings of SCION, DESKEW and INTERP are given in Appendix F.5.

In step (c) SCION first prints the virtual-height data to be analysed, and writes it to an output file (on unit 7) for plotting purposes. POLAN is then called to carry out the real-height analysis, using the standard default modes. The type of analysis can be adjusted if required by altering the parameter AMODE in Section (G) of SCION; the use of AMODE is described in Section 10.2.1. During the analysis POLAN produces some printed output relating to the overall layer parameters; this is described in Section 10.3.2. After the analysis SCION lists the height, frequency points which define the calculated real-height profile. These results are also written to a computer file (unit=7) for plotting and interpretation.

## 11.2 Entering Initial Specifications

Throughout this section the digitizer should be in the "INTERNAL" mode, in which data are accepted directly from the keyboard. The display shows appropriate prompts at each stage to indicate the type of entry required.

The digitization procedure is initiated by the normal END, EXECUTE, RUN PROGRAM sequence on the HP9821A. The digitizing program first gives the prompt "HEADER", to remind the user to enter data describing the ionogram. This prompt may be ignored if desired, provided the appropriate 4 lines [(1) to (4) below] are added to the file NHDATA before its use by SCION.

PROMPT:           HEADER???

Before any digitization has taken place, the terminal will be in the INTERNAL mode. If a previous ionogram has just been finished, switch from EXTERNAL to INTERNAL mode. Four lines of text should now be entered, corresponding to the first four READ instructions of SCION as detailed below.

(1)    READ (6,901) IEXIT, HEADC           -   in FORMAT (I4, 19A4).

Use IEXIT = 1 if another ionogram is to be digitized, and IEXIT = 0 if all required ionograms have been digitized. IEXIT = 0 causes a normal stop of SCION. The 19A4 format is for any descriptive header HEADC, and is usually left blank if IEXIT = 0.

(2)    READ (6,902) DIP, FB, START         -   in FORMAT (3F5.2).

DIP is the magnetic dip angle in degrees. FB is the gyrofrequency at ground level (in MHz), given by  $FB = 2.80 B$  where B is the magnetic field strength in gauss (1 gauss =  $10^{-4}$  Tesla). POLAN assumes an inverse-cube variation of FB with height. Values of DIP and of the gyrofrequency FH at 200 km height can be obtained from the Atlas of Ionograms (report UAG-10). To use the height-varying gyrofrequency in POLAN, the ground value is calculated from  $FB = 1.097 FH$ . If a constant gyrofrequency FH is to be used at all heights, this value is entered as  $FB = -FH$ .

START is normally an assumed (model) real height at a plasma frequency of 0.5 MHz. Selection of a value for START is discussed in Sections 6.3 and 10.5.

(3)    READ (6,904) (FM(I), I = 1,20)     -   in FORMAT (20F4.0).

This input specifies from 2 to 20 frequency marker values, in MHz, whose positions are to be digitized. The scale is assumed linear-in- $\ln(f)$  if only two markers are specified. Otherwise a four-point polynomial interpolation of  $\ln(f)$  is used for the frequency scale. The markers actually digitized must correspond to those specified here, in number and in frequency. A common input sequence at this point will be 1, 2, 4, 8, 16.

(4)    READ (6,904) (HM(I), I = 1,20)     -   in FORMAT (12F5.0).

Specify from 2 to 20 height marker values, in km, whose positions are to be digitized. The scale is assumed linear if only two markers are specified. With additional markers a 4-point height interpolation is used. The markers digitized must correspond to those specified here, in number and in height. If the height scale of the ionograms is accurately linear, the input here could be 100, 600. If there is any doubt about the height linearity a better sequence would be 0, 200, 400, 600.

## 11.3 Defining the Ionogram Coordinates

The digitizer is now switched to "EXTERNAL" and all further input is taken from the digitizing table. "End-of-layer" and "End-of-ionogram" information is entered by scaling points outside the normal area of the ionogram, as described below and in Section 11.4. The image or tracing to be scaled is of the general form shown in Fig. 26. In preparing a tracing, particular care must be taken in accurately identifying and tracing initial sections of the ordinary (O) and extraordinary (X) echoes. The corners (1) to (3) in Fig. 26 are formed by the intersection of two height markers, and two frequency markers or interference bands. The area to the bottom left of corner 1, called 'OFF-SCALE', is used to terminate each digitizing sequence. Areas to the top left of corner 2 and to the top right of corner 3 indicate the end of data from a given ionospheric layer. The corner areas must lie outside the area covered by the ionogram itself.

After scaling of the height markers, and switching the digitizer to EXTERNAL, the display shows

PROMPT: CORNERS?

Move the cursor well into the "off-scale" region (far bottom left) and press the "0" button. Then digitize the positions of the four corners of the tracing, clockwise from bottom left. These four points are used to "deskew" all later coordinates. Finally, digitize another "off-scale" point. This produces the next prompt:

PROMPT: FREQUENCY MARKERS?

Digitize the position of all frequency markers previously specified. The height at which the markers are digitized is not directly relevant. Using the points where the frequency markers cross the 200 km height line will generally give maximum accuracy with distorted ionograms. After 6 values have been entered, a carriage return is automatically inserted and the same prompt given again. After all the markers have been digitized, digitize an "off-scale" point; this will cause the next prompt:

PROMPT: HEIGHT MARKERS?

Digitize the position of all height markers previously specified. Again it is preferable to record the height markers at some frequency near the center of the section of the ionogram to be scaled. The marker series is terminated with another "off-scale" point.

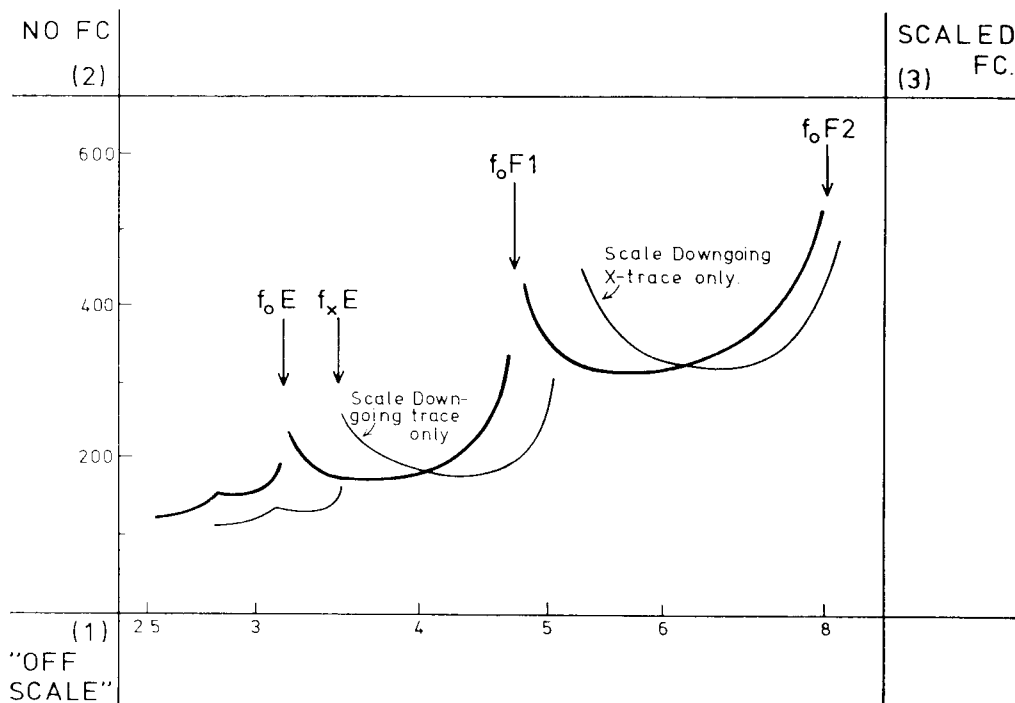


Figure 26. An ionogram showing separate E, F1 and F2 layers, and the corner areas used to pass information to the digitiser program.



## 11.4 Scaling the Ionogram

### 11.4.1 Entry of ordinary ray data

PROMPT:           0 TRACE?

Ionogram scaling normally begins at the lowest observed ordinary (O) ray frequency  $f_{min}$ . The first few points are scaled at a frequency interval of about 0.1 MHz. Thereafter the interval may be increased, to 0.2 MHz or more, in regions where the virtual height is changing slowly. Enough data points should be digitized to permit accurate reproduction of the virtual height curve. Suggested rules for the selection of data to be scaled are summarised in Section 10.4.2.

Digitizing continues up to the critical frequency defining the end of the first layer ( $f_oE$  in Fig 26). If the critical frequency can be defined accurately using traces from both the E and F layers it should be scaled, at any convenient height. The end of data from layer 1 is then indicated by scaling a point to the top right of corner (3). If the critical frequency is not scaled, end of data for layer 1 is indicated by scaling a point to the top left of corner (2).

For multi-layer ionograms, the second (F-layer) trace is digitised from just above  $f_oE$  up to the next critical frequency. This is normally  $f_oF2$ , although there may occasionally be a true discontinuity, and a critical frequency, at  $f_oF1$  (as in Fig. 26). Scaling of the second layer terminates with a "top left" point if the critical frequency is not scaled, or a "top right" point if the critical frequency is scaled.

Any additional layers are scaled in the same way, each data set terminating with a "top right" or "top left" point according as  $f_c$  was or was not scaled. Finally, the end of the ordinary ray data is shown by digitizing an "off-scale" point. The digitizer program will then display a prompt for extraordinary ray data.

### 11.4.2. Entry of extraordinary ray data.

After the "off-scale" point signalling the end of O-ray data, any useful X-ray data should be scaled. The selection of 'useful' data is discussed in Section 10.4.3. For start calculations, 6 to 8 points are scaled at the low-frequency end of the X-ray trace, using a frequency interval of about 0.1 to 0.05 MHz. When X data are scaled, SCION can incorporate this correctly only if it can identify each of the layers used in the O ray scaling. So if there are no useful X data for one layer, two "top-left" points must be digitized. When useful X data are available they are digitized normally and terminated with either

- (a) a "top-left" point if the trace does not give a useful estimate of the critical frequency  $f_{cx}$ ,
- or
- (b) scaling of the critical frequency followed by a "top-right" point.

Thus at least two points are digitized for each layer, even if the X trace is not present. Any scaled critical frequencies provide additional input for the least-squares peak calculation in POLAN.

The digitizer program assumes that O data have been scaled for three layers, called for convenience the E, F1 and F2 layers. Separate prompts are given for each layer, to help the operator in correctly terminating each data set. Data are digitized in order for each of the layers which were scaled with the O ray. Thus when only the night-time F layer is present, X-ray data for this layer are scaled in response to the first ("E-LAYER X?") prompt, and scaling is then terminated with an "off-scale" point.

Completion of the O-trace scaling by digitizing an "off-scale" point gives the first X-trace prompt:

PROMPT           E-LAYER X?

If there is a suitable E-layer X-mode trace present for daytime ionograms, OR a suitable F-layer X-mode trace present for night-time ionograms, digitize 5 to 9 points on the initial part of the trace using a frequency interval of 0.1 to 0.05 MHz. If the X-trace gives a reasonable estimate of the (X-mode) critical frequency, this frequency should next be digitized followed by a "top-right" point. If the critical frequency is not scaled, terminate the data for the first layer with a "top-left" point.

PROMPT F1-LAYER X?

If there was no second layer in the O-ray data, digitizing is terminated with an "off-scale" point. If the O data included a second layer, but there is no X-trace for this layer, digitize a "top-left" point; this is followed by an "off-scale" point if there are no further layers, or a second "top-left" point if a third layer is present.

When a suitable X trace is present for the second layer, digitize 5 to 9 points on the initial (downgoing) part of the trace. Finally digitize the X trace critical frequency and a "top-right" point, OR digitize a "top-left" point only.

PROMPT F2-LAYER X?

Repeat the above digitizing sequence for any third layer. Note that the F1 and F2 portions of an ionogram should be treated as two separate layers only if they are truly separated, with an intervening valley. This occurs only when the F1 trace tends to a vertical asymptote (at foF1) and is not connected to the F2 trace, as in Fig. 26. In the example of Fig. 24 (Section 10.4.1) there is only one F layer.

PROMPT HEADER???

Switch to INTERNAL and proceed as in (1) of Section 11.2. Thus if another ionogram is to be digitized, or the same one digitized again, key in the value one for IEXIT. Otherwise set IEXIT = 0 to terminate.

This completes the ionogram scaling.

## REFERENCES

- Becker, W. (1967), On the manual and digital computer methods used at Lindau for the conversion of multifrequency ionograms to electron density-height profiles, *Radio Sci.*, 2, 1205-1232.
- Becker, W. (1978), Conversion methods for  $h'(f)$  to  $N(h)$  used at Lindau, Appendix C of McNamara 1978(b).
- Budden, K.G. (1955), A method for determining the variation of electron density with height ( $N(z)$  curves) from curves of equivalent height against frequency ( $(h',f)$  curves), *Physics of the Ionosphere*, Rept. Phys. Soc. Conference, 332-339 (Phys. Soc. London).
- Douppnik, J.R. and E.R. Schmerling (1965), The reduction of ionograms from the bottomside and topside, *J. Atmosph. Terr. Phys.*, 27, 917-942.
- Ellis, G.R. (1957), Measurement of the gyrofrequency in the F region, *J. Atmosph. Terr. Phys.*, 11, 54-58.
- Gulyaeva, T.L. (1972), On a non-ambiguous statement of the problem of computing the  $N(h)$  profiles of the bottomside ionosphere, *Geomagnetism and Aeronomy*, 12, 551-553.
- Gulyaeva, T.L. (1973), Computation of  $N(h)$  profiles using the first and second order methods with a variable parameter in unobserved regions, in "Methods of computation and investigations of ionospheric  $N(h)$  profiles", edited by B.S. Shapiro, T.L. Gulyaeva, and N.I. Potapova, Moscow, IZMIRAN, p.76-99.
- Gulyaeva, T.L., W. Becker, L.F. McNamara, A.K. Paul, J.E. Titheridge and J.W. Wright (1978), Analysis of numerical ionograms. 2. The Starting Problem, *Ionospheric Prediction Service Series X Reports IPS-X7*, Sydney, Australia.
- Howe, H.H. and D.E. McKinnis (1967), Ionospheric electron density profiles with continuous gradients and underlying ionization corrections, 2. Formulation for a digital computer, *Radio Sci.*, 2, 1135-1158.
- Koehler, J.A. and L.F. McNamara (1975), Frequency and virtual height errors in I.P.S. Ionograms, *Ionospheric Prediction Service Series R Reports*, IPS-R29, Sydney, Australia.
- Knight, P. (1972), A classification of night-time electron-density profiles, *J. Atmosph. Terr. Phys.*, 34, 401-410.
- Lobb, R.J. and J.E. Titheridge (1977a), The valley problem in bottomside ionogram analysis, *J. Atmosph. Terr. Phys.*, 39, 35-42.
- Lobb, R.J. and J.E. Titheridge (1977b), The effects of travelling ionospheric disturbances on ionograms, *J. Atmosph. Terr. Phys.* 39, 129-138.
- Lockwood, G.E.K. (1969), A computer-aided system for scaling topside ionograms, *Proc. Inst. Elect. Electronics Eng.*, 57, 986-989.
- Lyon, A.J. and A.J.G. Moorat (1956), Accurate height measurements using an ionospheric recorder, *J. Atmosph. Terr. Phys.*, 8, 309-317.
- McNamara, L.F. (1976), The accuracy of the single polynomial method of ionogram analysis, *Ionospheric Prediction Service Series R Reports*, IPS-R32, Sydney, Australia.
- McNamara, L.F. and J.E. Titheridge (1977), Numerical ionograms for comparing methods of  $N(h)$  analysis, *Ionospheric Prediction Service Series X Reports*, IPS-X5, Sydney, Australia.
- McNamara L.F. (1978a), Ionospheric D-region profile data base, Report UAG-67, World Data Centre A for Solar Terrestrial Physics, NOAA, Boulder, CO 80303.
- McNamara L.F. (1978b), A comparative study of methods of electron density profile analysis, Report UAG-68, World Data Centre A for Solar Terrestrial Physics, NOAA, Boulder, CO 80303.
- McNamara L.F. (1978c), Selected disturbed D-region electron density profiles, Report UAG-69, World Data Centre A for Solar Terrestrial Physics, NOAA, Boulder, CO 80303.
- McNamara, L.F. (1979), Model starting heights for  $N(h)$  analyses of ionograms, *J. Atmosph. Terr. Phys.*, 41, 543-548.
- McNamara L.F. (1982), An Operational system for  $N(h)$  analysis of vertical incidence ionograms, Internal Report, Ionospheric Prediction Service, Sydney, Australia.
- Paul, A.K. (1960), Bestimmung der wahren aus der scheinbaren reflexionshohe, *Arch. Elek. Ubertragung*, 14, 468-476.
- Paul, A.K. and J.W. Wright (1963), Some results of a new method for obtaining ionospheric  $N(h)$  profiles with a bearing on the structure of the lower F region, *J. Geophys. Res.*, 68, 5413-5420.
- Paul, A.K. (1967), Ionospheric electron-density profiles with continuous gradients and underlying ionization corrections. I. The mathematical-physical problem of real-height determination from ionograms, *Radio Sci.*, 2, 1127-1133.
- Paul, A.K. and G.H. Smith (1968), Generalization of Abel's solution for both magnetoionic components in the real-height problem, *Radio Sci.*, 3, 163-170.
- Paul, A.K. (1977), A simplified inversion procedure for calculating electron density profiles from ionograms for use with minicomputers, *Radio Sci.*, 12, 119-122.

- Paul, A.K., T.L. Gulyaeva, L.F. McNamara, J.E. Titheridge and J.W. Wright. (1978), Analysis of numerical ionograms. 3. The valley problem, Ionospheric Prediction Service Series X Reports, IPS-X8, Sydney, Australia.
- Piggott, W.R. and K. Rawer (1972), U.R.S.I. handbook of ionogram interpretation and reduction, Report UAG-23, National Geophysical and Solar-Terrestrial Data Centre, NOAA, Boulder, CO 80303.
- Robinson, B.J. (1958), Ph.D. Thesis, University of Cambridge.
- Shinn, D.H. and H.A. Whale (1952), Group velocities and group heights from the magneto-ionic theory, J. Atmosph. Terr. Phys. 2, 85-105.
- Thomas, J.O. (1959), The distribution of electrons in the ionosphere, Proc. IRE., 47, No.2, 162-175.
- Titheridge, J.E. (1959a), Ray paths in the ionosphere; approximate calculations in the presence of the earth's magnetic field, J. Atmosph. Terr. Phys., 14, 50-62.
- Titheridge, J.E. (1959b), The use of the extraordinary ray in the analysis of ionospheric records, J. Atmosph. Terr. Phys., 17, 110-125.
- Titheridge, J.E. (1959c), Ionisation below the night-time F layer, J. Atmosph. Terr. Phys., 17, 126-133.
- Titheridge, J.E. (1961a), A new method for the analysis of ionospheric h'(f) records, J. Atmosph. Terr. Phys., 21, 1-12.
- Titheridge, J.E. (1961b), The effect of collisions on the propagation of radio waves in the ionosphere, J. Atmosph. Terr. Phys., 22, 200-217.
- Titheridge, J.E. (1966), The calculation of the heights of the peaks of the ionospheric layers, J. Atmosph. Terr. Phys., 28, 267-269.
- Titheridge, J.E. (1967a), Calculation of the virtual height and absorption of radio waves in the ionosphere, Radio Science 2, 133-138.
- Titheridge, J.E. (1967b), The overlapping-polynomial analysis of ionograms, Radio Science, 2, 1169-1175.
- Titheridge, J.E. (1969), The single polynomial analysis of ionograms, Radio Science 3, 41-51.
- Titheridge, J.E. (1974a), FORTRAN program LAPOL for the 5-term overlapping polynomial analysis of ionospheric virtual height records, Technical Report 74/2, Radio Research Centre, The University of Auckland, New Zealand.
- Titheridge, J.E. (1974b), Direct analysis of ionograms at magnetic dip angles of 26 to 30 degrees, J. Atmosph. Terr. Phys., 36, 575-582.
- Titheridge, J.E. (1975a), The relative accuracy of ionogram analysis techniques, Radio Science, 10, 589-599.
- Titheridge, J.E. (1975b), The analysis of night-time ionograms, J. Atmosph. Terr. Phys., 37, 1571-1574.
- Titheridge, J.E. and Lobb, R.J. (1977), A least-squares polynomial analysis and its application to topside ionograms, Radio Science 12, 451-459.
- Titheridge, J.E. (1978), The generalised polynomial analysis of ionograms, Technical Report 78/1, Radio Research Centre, The University of Auckland, New Zealand.
- Titheridge, J.E., W. Becker, L. Bossy, T.L. Gulyaeva, L.F. McNamara, and A.K. Paul (1978), Analysis of numerical ionograms. 1. Complete monotonic profiles and problems associated with the analysis of their ionograms, Ionospheric Prediction Service Series X reports, IPS-X6, Sydney, Australia.
- Titheridge, J.E. (1979), Increased accuracy with simple methods of ionogram analysis, J. Atmosph. Terr. Phys., 41, 243-350.
- Titheridge, J.E. (1982), The stability of ionogram analysis techniques, J. Atmosph. Terr. Phys., 44, 657-669.
- Titheridge, J.E. (1985a), Ionogram analysis: Least squares fitting of a Chapman-layer peak, Radio Science 20, 247-256.
- Titheridge, J.E. (1985b), Starting models for the real height analysis of ionograms, J. Atmosph. Terr. Phys., in press.
- Wright, J.W. (1967), Ionospheric electron-density profiles with continuous gradients and underlying ionization corrections. III. Practical procedures and some instructive examples, Radio Sci., 2, 1159-1168.
- Wright, J.W., A.K. Paul and E.A. Mechtly (1975), Electron density profiles from ionograms: Underlying ionization corrections and their comparison with rocket results, Radio Sci., 10, 255-270.